Geological Society, London, Special Publications

Understanding tsunamis, potential source regions and tsunami-prone mechanisms in the Eastern Mediterranean

S. Yolsal, T. Taymaz and A. C. Yalçiner

Geological Society, London, Special Publications 2007; v. 291; p. 201-230
doi:10.1144/SP291.10

Understanding tsunamis, potential source regions and tsunami-prone mechanisms in the Eastern Mediterranean

S. YOLSAL[1], T. TAYMAZ[1] & A. C. YALÇINER[2]

[1]*Department of Geophysical Engineering, Seismology Section, the Faculty of Mines, Istanbul Technical University, Maslak TR-34469, Istanbul, Turkey (e-mail: yolsalse@itu.edu.tr)*

[2]*Department of Civil Engineering, Ocean Engineering Research Centre, Middle East Technical University, TR-06531, Ankara, Turkey*

Abstract: Historical tsunamis and tsunami propagation are synthesized in the Eastern Mediterranean Sea region, with particular attention to the Hellenic and the Cyprus arcs and the Levantine basin, to obtain a better picture of the tsunamigenic zones. Historical data of tsunami manifestation in the region are analysed, and compared with current seismic activity and plate interactions. Numerical simulations of potential and historical tsunamis reported in the Cyprus and Hellenic arcs are performed as case studies in the context of the nonlinear shallow-water theory. Tsunami wave heights as well as their distribution function are calculated for the Paphos earthquake of 11 May 1222 and the Crete earthquake of 8 August 1303 as illustrative examples depicting the characteristics of tsunami propagation, and the effects of coastal topography and near-shore amplification. The simulation studies also revealed that the long-normal distributions are compatible with reported damage. Furthermore, it is necessary to note that high-resolution bathymetry maps are a crucial component in tsunami wave simulations, and this aspect is rather poorly developed in the Eastern Mediterranean. The current study also demonstrates the role of bottom irregularities in determining the wave-height distribution near coastlines. Assuming the probability of occurrence of destructive tsunamigenic earthquakes, these studies will help us to evaluate the tsunami hazard for the coastal plains of the Eastern Mediterranean Sea region. We suggest that future oceanographic and marine geophysical research should aim to improve the resolution of bathymetric maps, particularly for the details of the continental shelf and seamounts.

The complexity of plate interactions and associated crustal deformation in the Eastern Mediterranean region is reflected in many destructive earthquakes that have occurred throughout its recorded history, many of which are well documented and studied. Catastrophic tsunamis have also been observed at most of the European coasts. The Eastern Mediterranean region, including the surrounding areas of western Turkey and Greece, is one of the most seismically active and rapidly deforming regions in the world. Thus, the region provides an excellent natural laboratory and offers a unique opportunity to improve our understanding of the complexities of continental tectonics in an active collisional orogen (Taymaz *et al.* 2004; Fig. 1). The major scientific observations from this natural laboratory have clearly helped us to better understand the tectonic processes in active collision zones, the mode and nature of continental growth, and the causes and distribution of seismic, volcanic and geomorphological events (e.g. tsunamis) and their impact on humans and civilization. A tsunami is a very large ocean- or sea-wave triggered by various large-scale disturbances of the ocean floor such as submarine earthquakes, volcanic activities or landslides. These waves have unusually long wavelength, in excess of 100 km, generated in the open ocean and transformed into a series of catastrophic oscillations on the sea surface close to coastal zones. At the vicinity of the earthquake source, multiple reflections owing to deep basins and partial wave trapping because of the complex sea-bottom morphology generate complicated wave-train patterns, and it is difficult to determine whether these are related to the source or path effects. On the other hand, there is a long record of tsunami occurrences and damaging tsunamis observed repeatedly in the oceans and seas. Future tsunamis could be even more catastrophic than past events, as a result of the increasing occupation of the coasts with the economic development of coastal countries in recent decades. Furthermore, protection from natural disasters and mitigation of their effects on the environment and societies are becoming more important issues throughout the world.

The seismicity of the Aegean and the Mediterranean regions in general has been recorded from the ancient world to the end of the Middle Ages by an

From: Taymaz, T., Yilmaz, Y. & Dilek, Y. (eds) *The Geodynamics of the Aegean and Anatolia.* Geological Society, London, Special Publications, **291**, 201–230.
DOI: 10.1144/SP291.10 0305-8719/07/$15.00

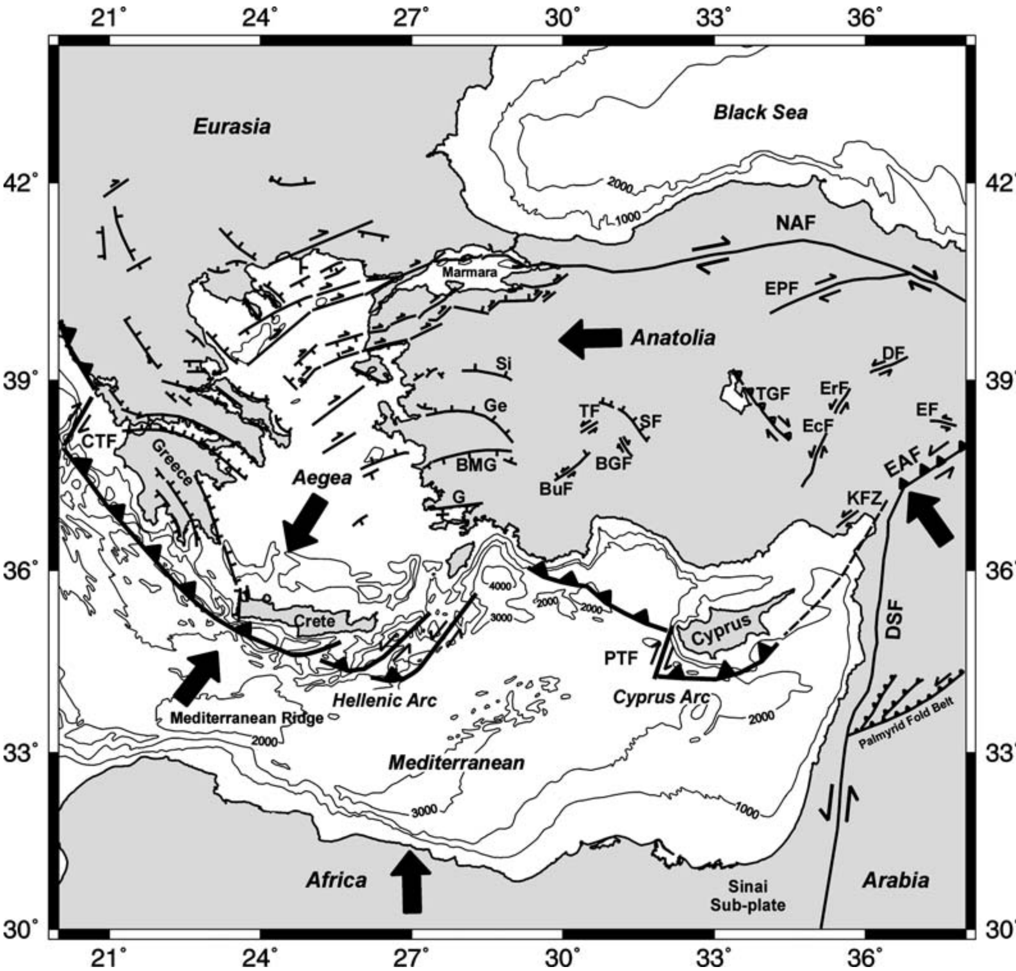

Fig. 1. Summary sketch map of the faulting and bathymetry in the Eastern Mediterranean Sea region, compiled from our observations and those of Le Pichon *et al.* (1984), Taymaz *et al.* (1990, 1991), Şaroğlu *et al.* (1992), Papazachos *et al.* (1998) and McClusky *et al.* (2000). NAF, North Anatolian Fault; EAF, East Anatolian Fault; DSF, Dead Sea Fault; EPF, Ezinepazarı Fault; PTF, Paphos Transform Fault; CTF, Cephalonia Transform Fault; G, Gökova; BMG, Büyük Menderes Graben; Ge, Gediz Graben; Si, Simav Graben; BuF, Burdur Fault; BGF, Beyşehir Gölü Fault; TF, Tatarlı Fault; SF, Sultandağ Fault; TGF, Tuz Gölü Fault; EcF, Ecemiş Fault; ErF, Erciyes Fault; DF, Deliler Fault; EF, Elbistan Fault; KFZ, Karataş–Osmaniye Fault Zone (see also Taymaz *et al.* 2007). Large black arrows show relative motions of plates with respect to Eurasia (McClusky *et al.* 2000, 2003). Bathymetric contours are shown at 1000 m interval, and are from GEBCO (1997) and Smith & Sandwell (1997*a*, *b*).

extraordinary wealth of written and epigraphic sources and this historical heritage is one of the most precious in the world. Thus, for the present study historical earthquakes and associated tsunamis are identified from verified catalogues (e.g. Guidoboni *et al.* 1994; Ambraseys & Melville 1995; Guidoboni & Comastri 2005*a*, *b*; Sbeinati *et al.* 2005). Understanding of the geometry and evolution of potential source (seismogenic) regions and the source rupture process along active zones has crucial implications for tsunami generation. Around the Mediterranean Sea, Marmara Sea and Black Sea there is a high potential risk for generation of tsunamis, and the most destructive events have occurred along the coasts of Portugal, Italy, Greece and Turkey. The impact of tsunamis on human societal life can be traced back in written history to late Minoan time (1600–1300 BC) in the Eastern Mediterranean, when the strongest tsunami caused by the volcanic eruption of Santorini resulted in degradation of the Minoan civilization, and it has been further concluded that this eruption and the following tsunami were widely observed on the coastal plains of western Turkey and Crete (Minoura *et al.* 2000). Hence, tsunamis have caused severe damage and flooded lowlands in many segments of the Mediterranean coasts. Historical documents, and geological, archaeological and many trench studies demonstrate that parts of the Turkish coastlines have suffered from disastrous sea-waves several times in the past (Yalçıner *et al.* 2002, 2004; Boschi *et al.* 2005; Guidoboni & Comastri 2005*a*, *b*; Scheffers & Kelletat 2005; Fokaefs & Papadopoulos 2006; Papadopoulos *et al.* 2007). The style of seismic deformation along the Cyprus and Hellenic arcs exhibits the characteristics and structural complexities associated with strike-slip, thrust and normal faulting as a result of convergence between the Aegean, Anatolia, Eurasia and Eastern Mediterranean lithosphere. Existing observations and inferred seismological results indicate that there are younger tectonic, slope failure features within the lower part of the continental slope that are tsunamis-prone locations along the neighbouring coastlines of the Mediterranean Sea

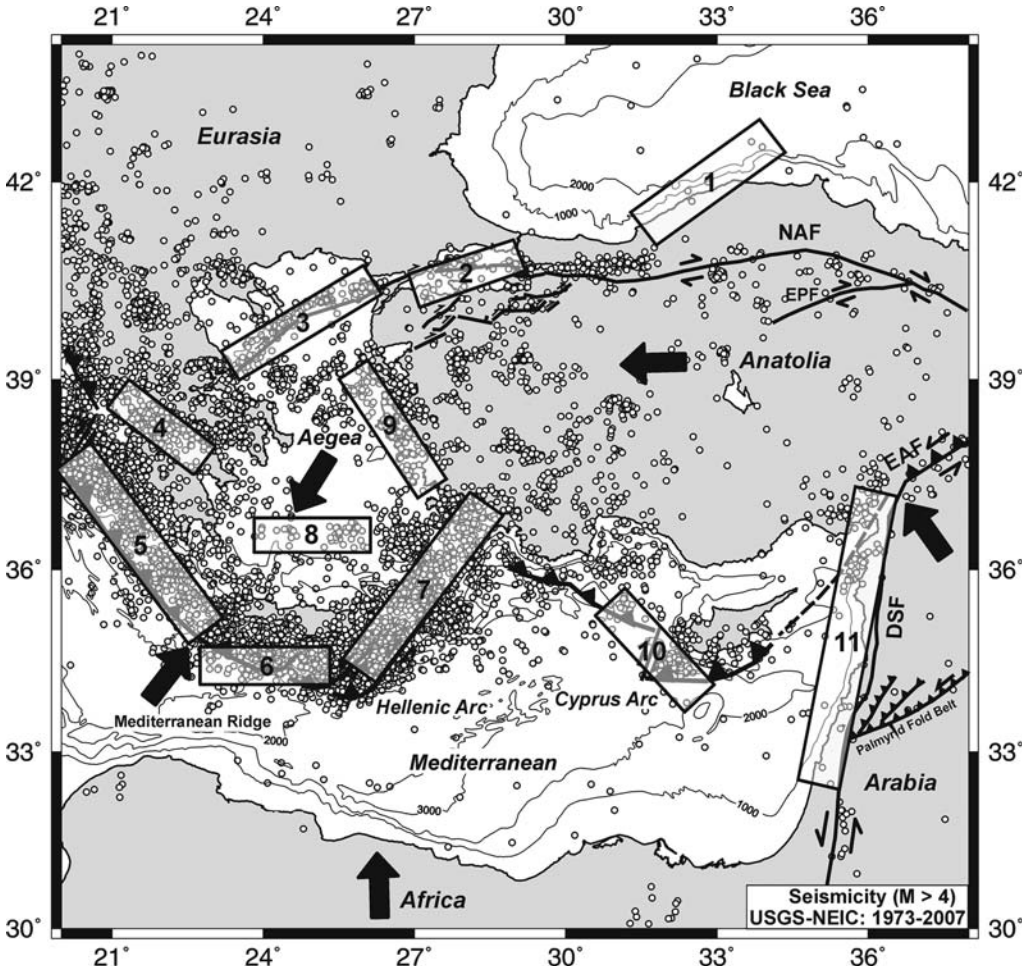

Fig. 2. A sketch map of the known tsunamigenic zones in the Eastern Mediterranean Sea region (see Tables A1–A3 for details). Rectangular boxes with numbers refer to the regions discussed in the text: 1, Bartın–Amasra shelf, SW Black Sea; 2, Sea of Marmara; 3, North Aegean trough; 4, Gulf of Corinth; 5, western Hellenic arc; 6, south of Crete; 7, eastern Hellenic arc; 8, the Cyclades; 9, Seferihisar-Kuşadası, W Turkey; 10, SW of Cyprus arc; 11, Dead Sea Fault Zone and Levantine Sea. Large black arrows show relative motions of plates with respect to Eurasia (McClusky *et al.* 2000, 2003). Bathymetric contours are shown at 1000 m interval, and are from GEBCO (1997). Seismicity of the region reported by USGS–NEIC during 1973–2007 for $M > 4$ is shown by small open circles. The display convention of major plate boundaries is the same as in Figure 1.

(Makris & Stobbe 1984; Taymaz *et al.* 1990, 1991; ten Veen *et al.* 2004; Yolsal & Taymaz 2004, 2005; Fig. 2). In addition to historical and geological information, and the distribution of active fault zones, volcanoes and other probable tsunami-prone sea-bottom morphological structures, there are numerous source regions that may be considered responsible for severe tsunamis. However, major tsunami recurrence in the Eastern Medierranean region is of the order of several decades and the memory of tsunamis is short lived. Thus, the compilation of reliable tsunami databases is of great importance for a wide range of tsunami research (e.g. statistics and hazard assessment, numerical modelling, risk assessment, early warning operations, public awareness).

Hence, we aim to concentrate on tsunami risk mapping for regions where no severe tsunami has occurred recently, but the geomorphological and topographic features, and the geodynamic and seismotectonic settings are similar to those of areas devastated by recent catastrophic tsunamis such as Sumatra (Barber *et al.* 2005) and where reliable historical records of tsunamis are available (Guidoboni & Comastri 2005*a*, *b*). In this paper, tsunami events known to have occurred in the Eastern Mediterranean Sea region are summarized, and synthetic tsunami simulations are presented as case studies to demonstrate preliminary tsunami risk estimates. Thus, this study deals only with earthquake-induced tsunamis.

Quantification of tsunamis

There have been considerable efforts early the 1930s to improve quantification of tsunamis observed globally (Sieberg 1932). However, this is still a puzzling aspect in tsunami research, as several intensity scales have been proposed to measure tsunami size (i.e. intensity and/or magnitude). On the other hand, earthquake magnitude is an objective physical parameter that defines the energy release radiated at the centroid, and does not directly reflect macroseismic effects although variable intensities at different geological locations can be observed. Nevertheless, Okal (1988) has already studied in detail the influence of the seismic source parameters (e.g. focal depth, source mechanism (geometry of faulting), seismic moment and directivity) on the generation of a tsunami, using the modal approach for laterally homogeneous, structural models. These boundary conditions certainly play an important role in defining the amplitude of tsunami waves, but so too do the other essential key parameters (i.e. the effects of the directivity as a result of rupture propagation along a fault, and enhanced tsunami excitation in a medium with weaker elastic properties, such as sedimentary layers). Thus, the quantification of tsunamis could easily be approached by analogy to general aspects of earthquake seismology (e.g: Abe 1979, 1981, 1985; 1989; Murty & Loomis 1980; Gasperini & Ferrari 2000; Papadopoulos & Fokaefs 2005; Papadopoulos & Satake 2005). In the Mediterranean region, tsunami intensity (k) is traditionally estimated using the Sieberg–Ambraseys scale (Ambraseys 1962), and tsunami magnitude (M_T or M_L) is generally calculated using the analytical formulae that have been developed (e.g. Murty & Loomis 1980). However, it should also be noted that the tsunami magnitude scales are usually based on direct measurements of tsunami wave heights at tide gauges located near coastlines. On the other hand, there are other effective parameters in tsunami generation such as coastal topography, variations in near-shore bathymetry, and the reflection, refraction, diffraction and resonance of sea-waves, to name a few. Thus, it is desirable to have a better calibration of analytical formulae based on both the quality and quantity of instrumental tide-gauge measurements.

Analysis of historical tsunamis in the Eastern Mediterranean

The descriptions of historical tsunamigenic earthquakes in the Eastern Mediterranean region are provided in valuable catalogues in various languages and recently compiled by Guidoboni & Comastri (2005*a*), who analysed sources in several languages (Greek, Latin, Arabic, Hebrew, Armenian, Italian, French, German, Ottoman and modern Turkish, etc.). Although the accounts of events gathered in catalogues cannot necessarily be described as definitive owing to the nature of research considered, they are very valuable documentation for researchers. Of course, the catalogues also contain much information on earthquakes, tsunamis, environmental effects, stories related to societal life and even religious belief, which should be carefully used by cross-correlating with other sources of information to gather self-consistent and complete datasets. Thus, in this study we have summarized tsunamigenic earthquakes in groups in the Appendix (Tables A1–A3) with relevant references.

In Figure 3, the locations of tsunamigenic earthquakes reported during the 11th–15th centuries in the Eastern Mediterranean region are plotted and are correlated with seismically active regions (see Table A1; Guidoboni & Comastri 2005*a*). Locations of tsunamigenic earthquakes

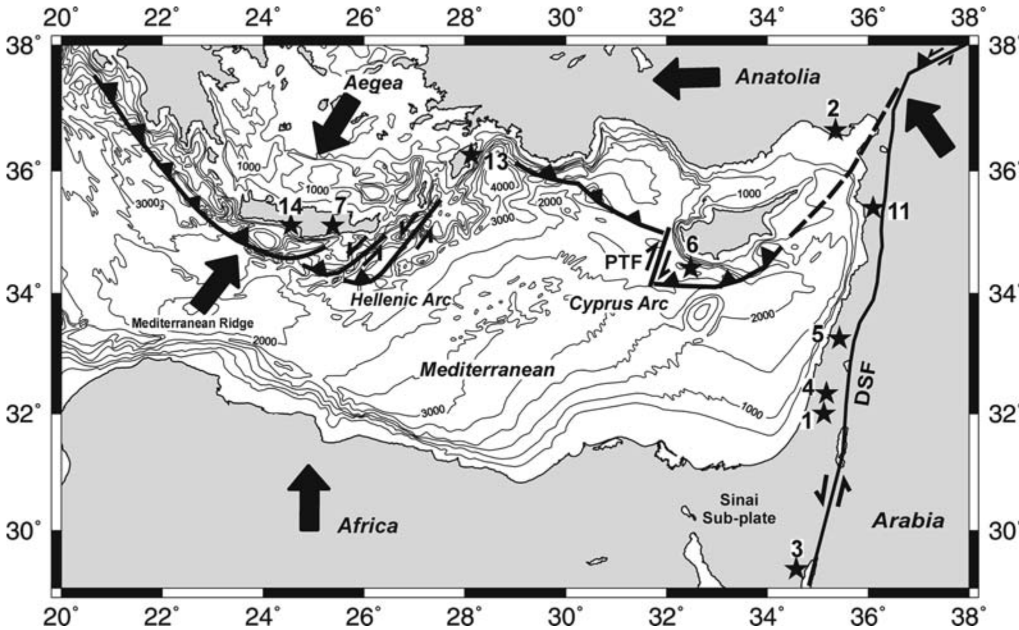

Fig. 3. Reported locations of tsunamigenic earthquakes during 11th–15th centuries in the Eastern Mediterranean Sea region (Guidoboni & Comastri 2005*a*). Large black arrows show relative motions of plates with respect to Eurasia (McClusky *et al.* 2000, 2003). Bathymetric contours are shown at 500 m interval, and are from GEBCO (1997). The display convention of major plate boundaries is the same as in Figure 1. Numbers refer to tsunamigenic events in Table A1.

reported in the Levantine basin and surrounding regions from 1365 BC to AD 1900 are shown in Figure 4, and a selected table of historical tsunamigenic earthquakes with estimated intensities at relevant locations and accompanying geomorphological effects are further summarized in Table A2 (see Sbeinati *et al.* 2005). It can be seen that there are about a dozen or so strong tsunami events in the Eastern Mediterranean, which reflects an apparent recurrence interval of about 150–200 years. It is also evident that tsunamigenic events are associated mainly either with seismogenic zones or with the active volcanic complex of Thera and seamounts of the Eastern Mediterranean Sea. However, some of the damaging historical tsunamis (e.g. 1303 and 1481) in the eastern Hellenic arc also threatened the coastal plains of the Cyprus, the Levantine and Alexandria–Nile Delta (Egypt) regions, and thus special care should be taken in evaluating of the tsunami risk of the region.

In Figure 5, locations of tsunamigenic earthquakes reported along the Hellenic arc and trench system are plotted, and they are correlated with relevant seismogenic zones (see Table A3; Papadopoulos *et al.* 2007).

Synthetic tsunami simulations

Geodynamic and seismotectonic setting

The Eastern Mediterranean Sea region is seismically active and its geodynamic and seismotectonic setting is mainly dominated by the Hellenic and the Cyprus arcs, the left-lateral strike-slip Dead Sea fault and the Levantine rift (Fig. 6). There are many historical documents available to correlate earthquakes and tsunamis along these seismogenic zones (e.g. Guidoboni *et al.* 1994; Ambraseys & Melville 1995; Papazachos *et al.* 1999; Guidoboni & Comastri 2005*a*, *b*; Sbeinati *et al.* 2005; Fokaefs & Papadopoulos 2006). In the Hellenic and Cyprus arcs crustal and intermediate-depth dip-slip faulting earthquakes often occur mostly in the submarine environment, and therefore damaging events are expected to generate strong tsunamis by co-seismic displacement. However, there are some cases where the generation mechanism of locally strong tsunamis associated with earthquakes reported clearly on land along the strike-slip Dead Sea fault and the Levantine rift remains unexplained. One possibility could be triggered slumping of unstable sediments on the shelf and/or

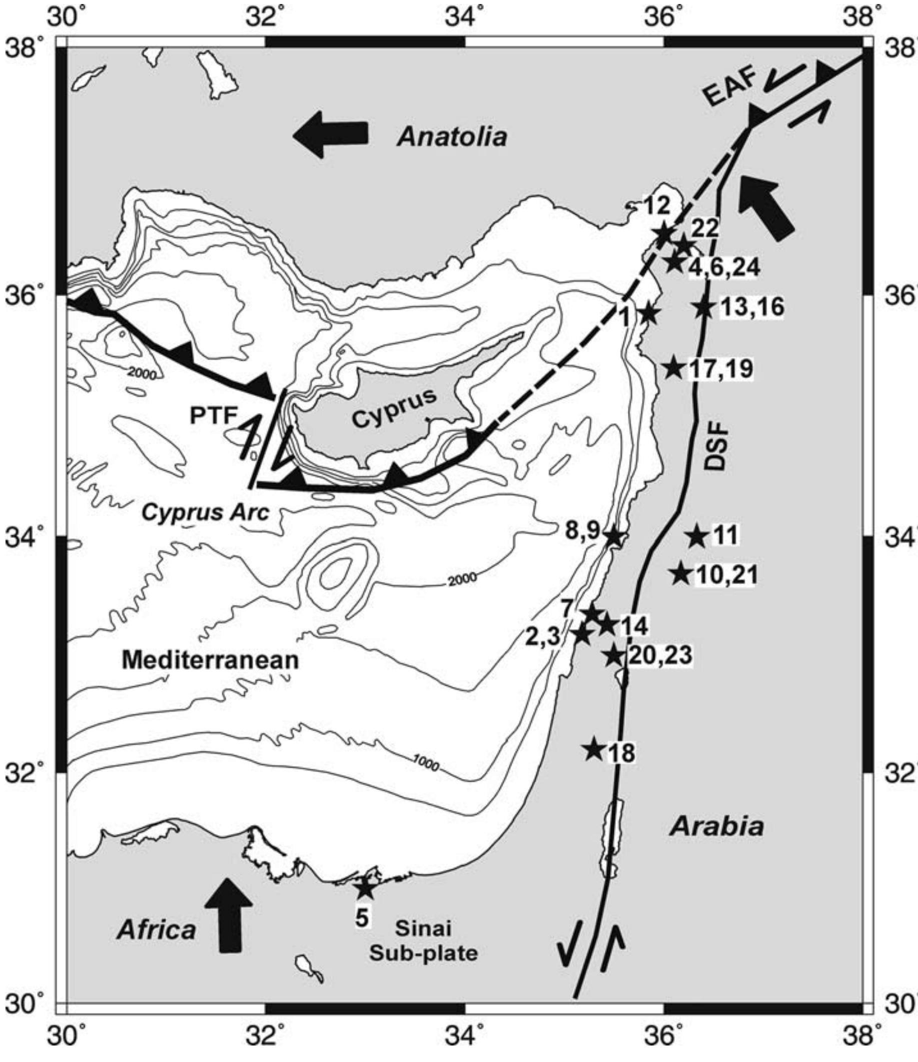

Fig. 4. Reported locations of tsunamigenic earthquakes in the Levantine basin and surrounding regions from 1365 BC to AD 1900 (Sbeinati *et al.* 2005). Large black arrows indicate relative motions of plates with respect to Eurasia (McClusky *et al.* 2000, 2003). Bathymetric contours are shown at 500 m interval, and are from GEBCO (1997). The display convention of major plate boundaries is the same as in Figure 1. Numbers refer to tsunamigenic events in Table A2.

propagating line-source and directivity effects of the rupture. It should also be noted that none of the reported tsunamis associated with seismic activity in the Dead Sea fault region propagated large distances. This may be due to very strong sea-wave attenuation, which is a known feature of landslide-generated tsunamis. In the Cyprus arc, earthquake activity is clearly recognized at offshore seismogenic zones west and SW of Cyprus, where tsunami generation by coseismic displacement in the submarine environment is possible (Figs 4 and 6). Therefore, tsunami potential and hazard in the Cyprus–Levantine region should not be neglected when considering the effects of the 1303 and 1481 tsunamis in the Hellenic arc (Tables A1–A3; Guidoboni & Comastri 2005*a*). In summary, the kinematics of the active sutures and plate boundaries and associated secondary structures in the Eastern Mediterranean Sea region is capable of generating damaging tsunamis.

In Figure 6, the seismicity of the Cyprus arc reported by the USGS–NEIC during 1973–2007

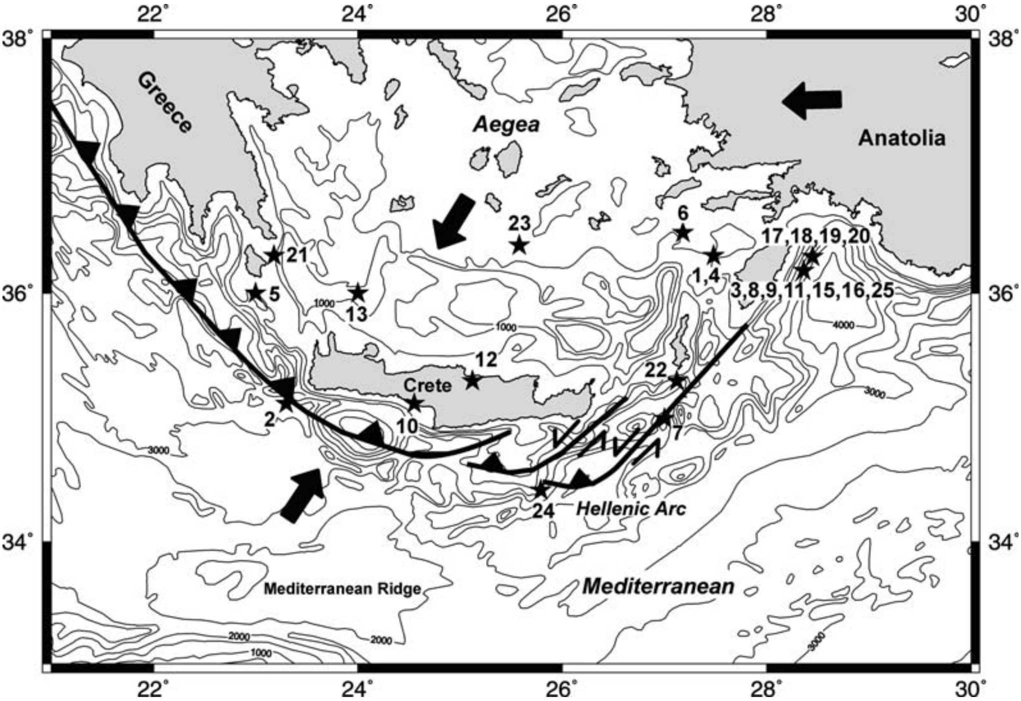

Fig. 5. Reported locations of tsunamigenic earthquakes along the Hellenic arc and trench system (Papadopoulos 2001; Papadopoulos *et al.* 2007). Large black arrows show relative motions of plates with respect to Eurasia (McClusky *et al.* 2000, 2003). Bathymetric contours are shown at 500 m interval, and are from GEBCO (1997). Major plate boundaries are as shown in Figure 1. Numbers refer to tsunamigenic events in Table A3.

for $M > 3$ is shown, including bathymetry data provided by GEBCO (1997). The current seismic activity is mainly concentrated on the southern flanks of the Troodos massif, and south and SW of Cyprus along the Paphos transform fault (PTF). The details of the clusters at crustal and intermediate depths and their source rupture properties have been described by Yolsal & Taymaz (2004, 2005). It is obvious from the distribution of histograms that not many large earthquakes ($M > 7$) have occurred in the region for about 30 years or so. This is not surprising when the recurrence periods in the historical catalogues of earthquakes and tsunamis are considered. Nevertheless, this region is capable of generating tsunamis by coseismic fault displacements provided that large earthquakes occur at relatively shallow depths.

The nonlinear shallow-water theory

Tsunamis are mainly generated by the sudden movement of the sea bottom as a result of submarine earthquakes, which causes long sea-waves for which the vertical acceleration of water particles is negligible compared with gravitational acceleration. The curvature of trajectories of water particles is relatively small except for oceanic propagation of a tsunami. Consequently, the vertical motion of water particles has no effect on the pressure distribution. Thus, it is a good approximation to assume that the pressure is hydrostatic. Furthermore, tsunami waves travel outwards in all directions from the source area, with the direction of the main energy propagation generally being orthogonal to the direction of the earthquake rupture zone, at various speeds depending on the depth of water propagated. Near shorelines, the tsunami-wave speed slows to just a few tens of kilometres per hour; however, the height of the waves increases to tens of metres. For the propagation of tsunami waves in shallow water, the horizontal eddy turbulence can be negligible compared with bottom friction except for the run-up on land. Therefore, it can be assumed that horizontal velocities of water particles are vertically uniform. In recent years, numerical models have been developed to simulate tsunami waves and their

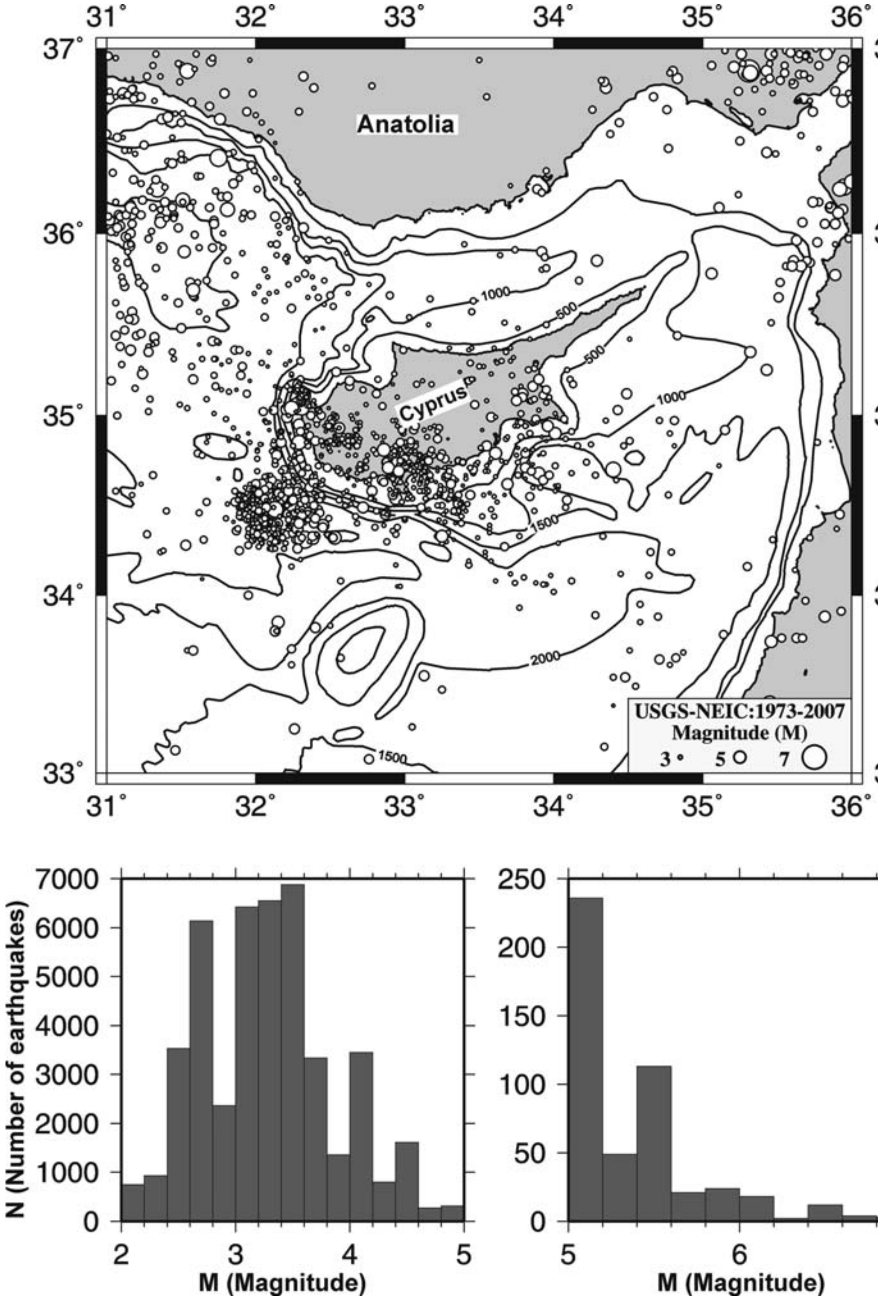

Fig. 6. Seismicity of the Cyprus arc and surroundings reported by USGS–NEIC during 1973–2007 scaled with respect to magnitudes for M > 3. Bathymetry data are derived from GEBCO/97-BODC, provided by GEBCO (1997) and Smith & Sandwell (1997*a*, *b*).

interaction with land masses based on long-wave equations with respect to related initial and boundary conditions. In the present study, the nonlinear shallow-water mathematical models TUNAMI-N2, AVI-NAMI and NAMI-DANCE are used to simulate the propagation of tsunami waves in the form

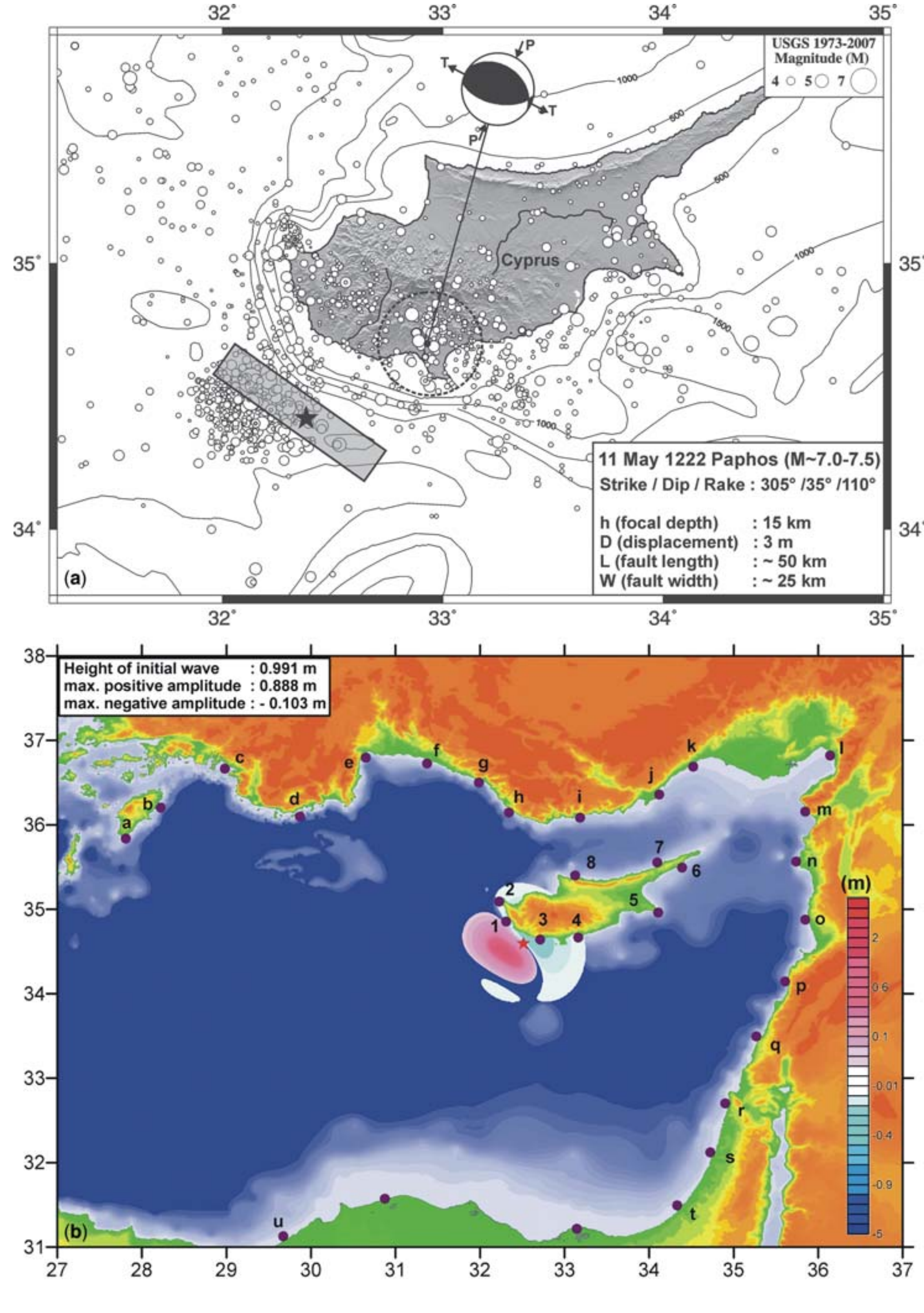

Fig. 7. (**a**) Seismicity of the Cyprus arc and surroundings as in Figure 6. Box with star refers to approximate location of the 11 May 1222 Paphos earthquake (M $\sim$ 7.5) and tsunami, for which simulations are generated by applying an analogous representative earthquake derived from teleseismic P- and SH-wave modelling studies of current earthquakes. The parameters of tsunami simulations are shown in the box in the lower right corner, and a representative fault-plane solution obtained from current earthquake source mechanisms is shown above in a lower hemisphere projection. (**b**) Snapshot of the initial tsunami generated with the parameters given in (a). Letters and numbers refer to geographical locations where macroseismic observations have been partly reported (Guidoboni & Comastri 2005*a*), and synthetic tsunami mareograms generated at pseudo-tide-gauge locations, and details are shown in Figure 8a and b.

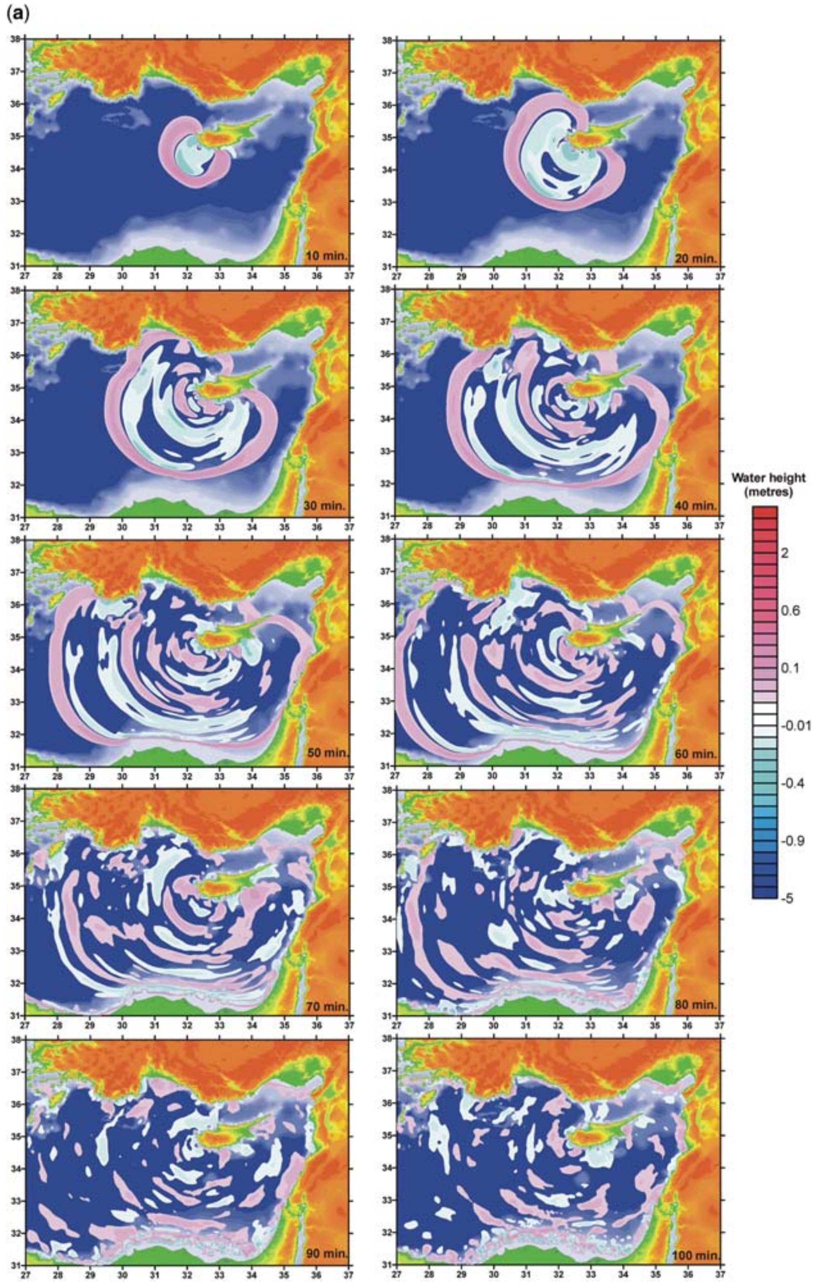

Fig. 8. (**a**) Snapshots of the tsunami wave propagation generated using nonlinear shallow-water theory for various times at 10 min intervals for the 11 May 1222 Paphos event. The water surface height is in metres and a colour scale is given on the right-hand side in metres. It should be noted that the bathymetric features of the Nile Delta (Fig. 7*b*) act as a natural barrier to slow down tsunami waves at shallower depths (<500 m) by refractions and diffractions of sea-waves. If we compare synthetic tsunami mareograms at 30, 40, 50 and 60 min, anomalous sea-wave heights are obvious at location *u* in (**b**) (Alexandria, Egypt), where there is *c*. 1 m mareogram amplitude. This could be due to a deep basin and sudden shelf break clearly reflected in the bathymetry. However, no significant sea-wave amplitudes were calculated at locations marked in (b) with filled circles and without letters. (b) Computed tsunami records at selected locations for the 11 May 1222 Paphos event. The vertical and horizontal scales show water surface elevation (wse) in centimetres and tsunami simulation time (t) in minutes, respectively. Above each tsunami mareogram, the maximum synthetic wave-heights (H) and theoretical arrival times (T) are given in centimetres and minutes, respectively.

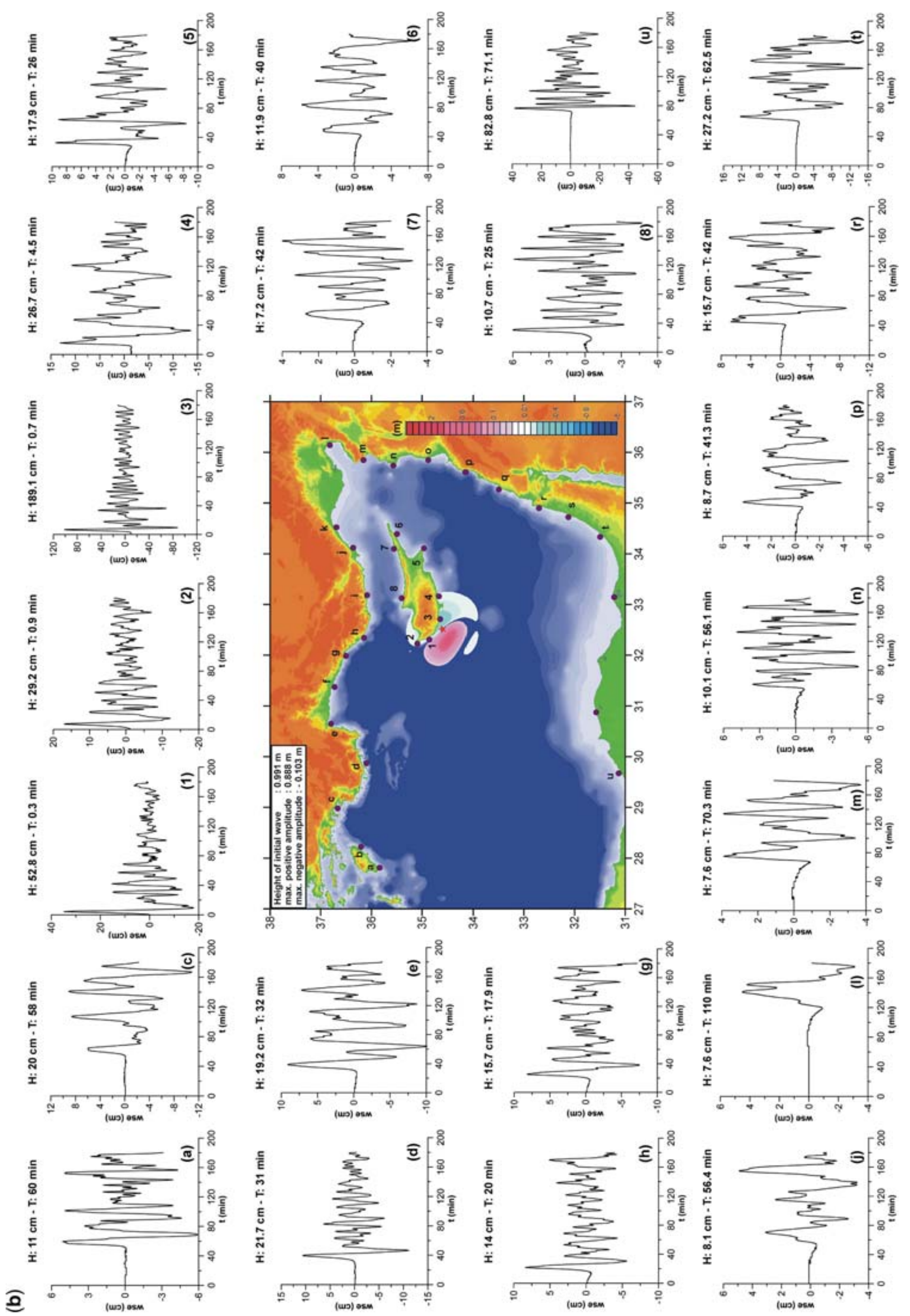

Fig. 8. *Continued.*

of Saint-Venant equations (Shuto *et al.* 1990; Pelinovsky *et al.* 2001; Zahibo *et al.* 2003; Yalçıner & Pelinovsky 2007).

Case studies

Paphos, Cyprus, 11 May 1222 (06:15 UT, latitude 34°42′N, longitude 32°48′E, Io = IX, Me ~ 7.0–7.5). In this section we present a case study of the 11 May 1222 Paphos, Cyprus earthquake and tsunami for which synthetic tsunami simulations are generated to analyse the importance of joint examination of earthquake source mechanism and tsunami simulation studies (Figs 6–8). The Paphos, Cyprus earthquake and related tsunami of 11 May 1222 is one of the most destructive events reported in many historical catalogues (Ergin *et al.* 1967; Ambraseys *et al.* 1994; Guidoboni & Comastri 2005*a*; Table A1). The towns of Limasol, Paphos and Nicosia were severely affected, especially Paphos, where the castle collapsed and there were many victims. The earthquake was also felt in regions as far as Alexandria (Egypt), and the harbour at Paphos was left completely without water.

The choice of the tsunami source is usually a complicated problem because it requires a good knowledge of the earthquake rupture mechanism. The related parameters for the 11 May 1222 Paphos event are adapted by analogy to current plate boundaries and earthquake source mechanisms obtained by inversion of teleseismic P- and SH-waveforms (Yolsal & Taymaz 2004, 2005). We have assumed that the initial wave elevation reflects instantaneously the bottom displacement, obtain rough estimates of the tsunami characteristics, although the earthquake magnitude, source depth and displacement are also critical parameters. However, the trade-off between the tsunami heights on different coastal plains should be more realistic, as it depends on the coastal topography and on very rough characteristics of the tsunami source (i.e. earthquake source orientation).

In the present study, we use the numerical models TUNAMI-N2 and AVI-NAMI based on the method of Okada (1985) for simulation and animation of tsunami generation and propagation, and of coastal amplification of nonlinear long waves in a given arbitrarily shaped bathymetry. TUNAMI-N2 and AVI-NAMI algorithms are the key tools for developing studies for the wave propagation and coastal amplification of tsunamis in relation to various initial conditions. The routines also compute the water surface fluctuations and velocities at all locations, even for shallow-water and land regions within the limitations of the bathymetric grid size used (Shuto *et al.* 1990; Goto *et al.* 1997; Yalçıner *et al.* 2003, 2004). The coseismic deformation is computed using an elastic dislocation model that yields the vertical deformation on the sea floor in the epicentral area as a function of the ground elastic parameters and the fault-plane geometry (Okada 1985). For the simulation, it is assumed that this deformation is instantaneous and fully transmitted to the sea surface. Hence, the earthquake source can then be modelled as a rupture of a single rectangular fault plane characterized by parameters describing location, orientation and rupture direction of the plane (i.e. rupture length, rupture width, focal depth, maximum displacement, strike, dip, rake angles). We have further gathered global bathymetric data provided by GEBCO (1987) and Smith & Sandwell (1997*a*, *b*) with a 1000 m grid size for the tsunami simulations and a time-step of $\Delta x/\Delta t = (2gh_{\max})^{1/2}$, where $h_{\max}$ and g are the maximum still water depth and gravitational acceleration, respectively, in a concept of stability to provide stable and meaningful results.

Figure 8a shows snapshots of the tsunami wave propagation generated using nonlinear shallow-water theory for various times at 10 min intervals for the 11 May 1222 Paphos event. It should be noted that the bathymetric features of the Nile Delta (Fig. 8a and b) act as a natural barrier to slow down tsunami waves at shallower depths (<500 m), as a result of refractions and diffractions of sea-waves. The effects of tsunami waves are clearly visible when synthetic tsunami simulations at 30, 40, 50 and 60 min are compared. Anomalous sea-wave heights are obvious at location *u* (Alexandria, Egypt), where there is *c.* 1 m mareogram amplitude (Fig. 8b). This could be due to a deep basin and sudden shelf break reflected in the coastal bathymetry. However, there are no significant sea-wave amplitudes calculated at locations marked with filled circles without letters. The computed water surface elevations (wse) and theoretical arrival times are presented at selected locations for the 11 May 1222 event in Figure 8b.

Crete, 8 August 1303 (03:30 UT, latitude 35°11′N, longitude 25°38′N, Io = X, Me ~ 8.0). The earthquake of 8 August 1303 proves to be one of the largest and best-documented seismic events in the history of the Mediterranean area. The effects of this earthquake and associated tsunami waves were very destructive and in many ways comparable with other reported events of 29 May 1508 (Ambraseys *et al.* 1994) and 12 October 1856 (Sieberg 1932; Ambraseys *et al.* 1994). It has been suggested that the epicentre was probably near the island of Crete, and

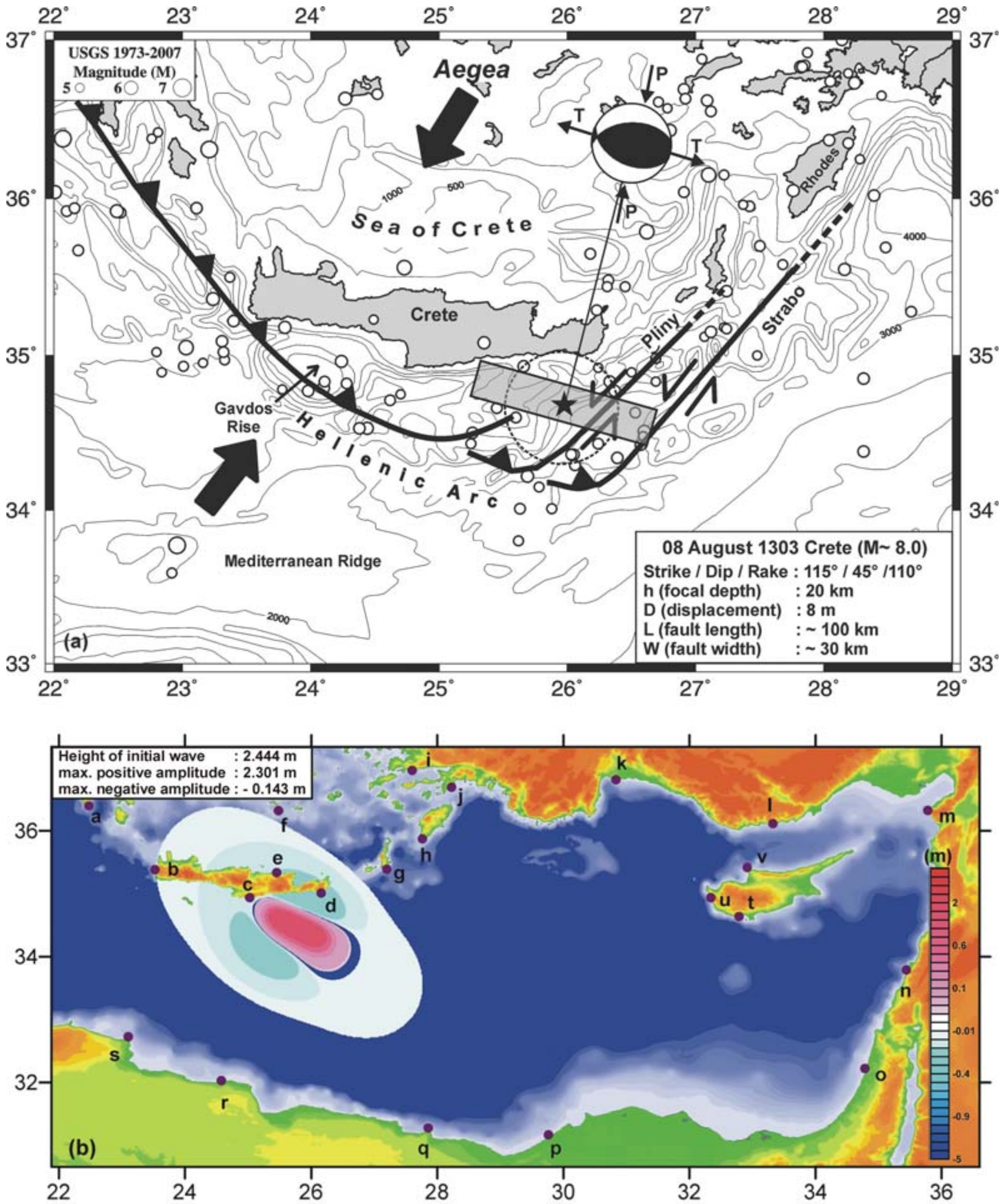

Fig. 9. (**a**) Seismicity of the Hellenic arc and surrounding region reported by USGS–NEIC for 1973–2007 scaled with respect to magnitudes for M > 5. The box with star indicates the approximate location of the 8 August 1303 Crete earthquake (M ~ 8.0) and tsunami, for which simulations are generated by applying an analogous representative earthquake derived from teleseismic P- and SH-wave modelling studies of current earthquakes. The parameters of tsunami simulations are shown in the box in the lower right corner, and a representative fault-plane solution obtained from current earthquake source mechanisms is shown above in a lower hemisphere projection. Large black arrows show relative motions of plates with respect to Eurasia (McClusky *et al.* 2000, 2003). Bathymetric contours are shown at 500 m interval, and are from GEBCO (1997). (**b**) Snapshot of the initial tsunami generated with the parameters given in (a). Letters and numbers refer to geographical locations where macroseismic observations were partly reported (Guidoboni & Comastri 2005*a*), and synthetic tsunami mareograms generated at pseudo-tide-gauge locations, and details are shown in Figure 10a and b.

(a)

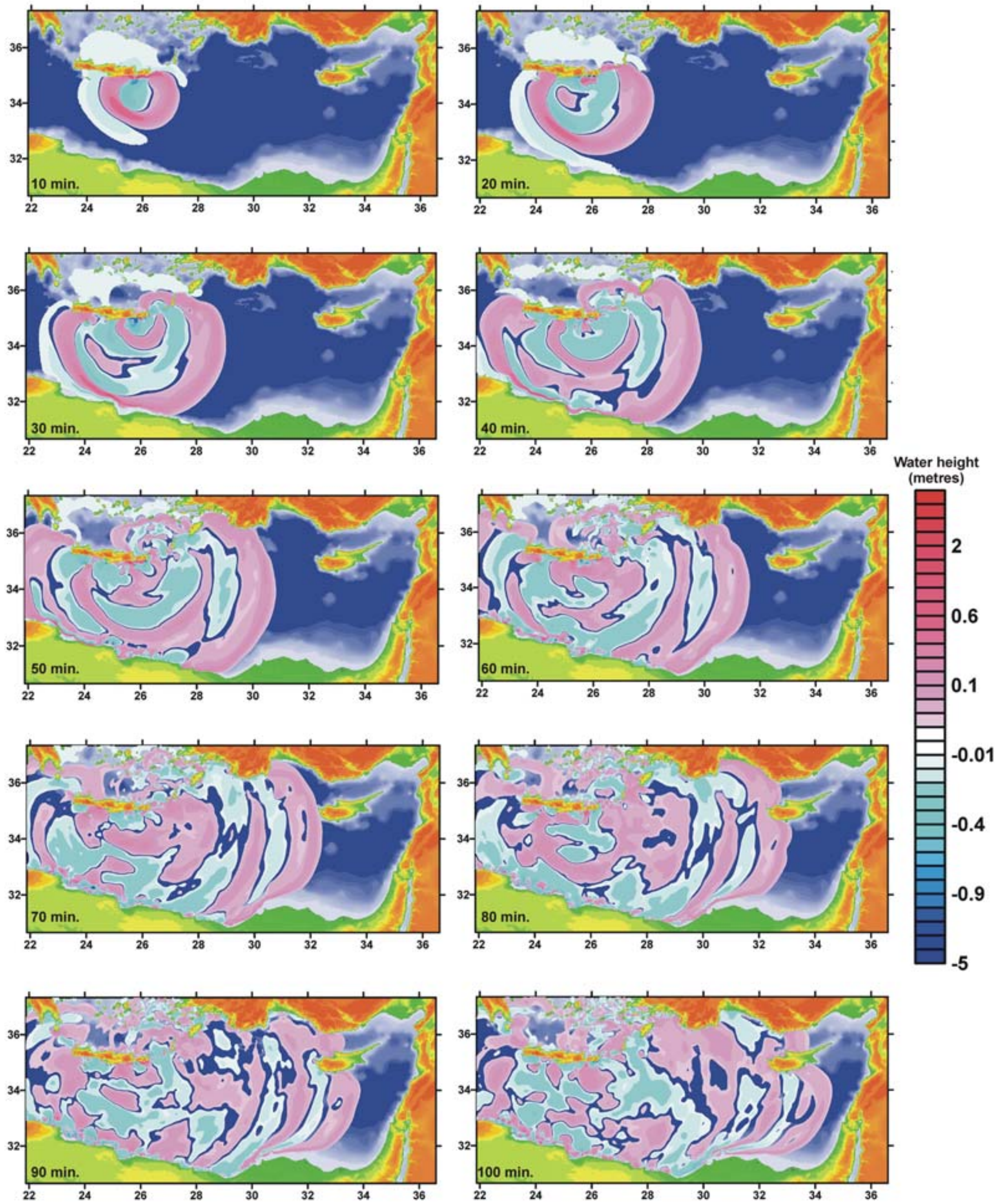

Fig. 10. (**a**) Snapshots of the tsunami wave propagation generated using nonlinear shallow-water theory for various times at 10 min intervals for the 8 August 1303 Crete event. The water surface height is in metres and a colour scale is given on the right-hand side in metres. (**b**) Computed tsunami records at selected locations for the 8 August 1303 Crete event. The vertical and horizontal scales show water surface elevation (wse) in metres and tsunami simulation time (t) in minutes, respectively. Above each tsunami mareogram are maximum synthetic wave-heights (H) and theoretical arrival times (T), given in centimetres and minutes, respectively.

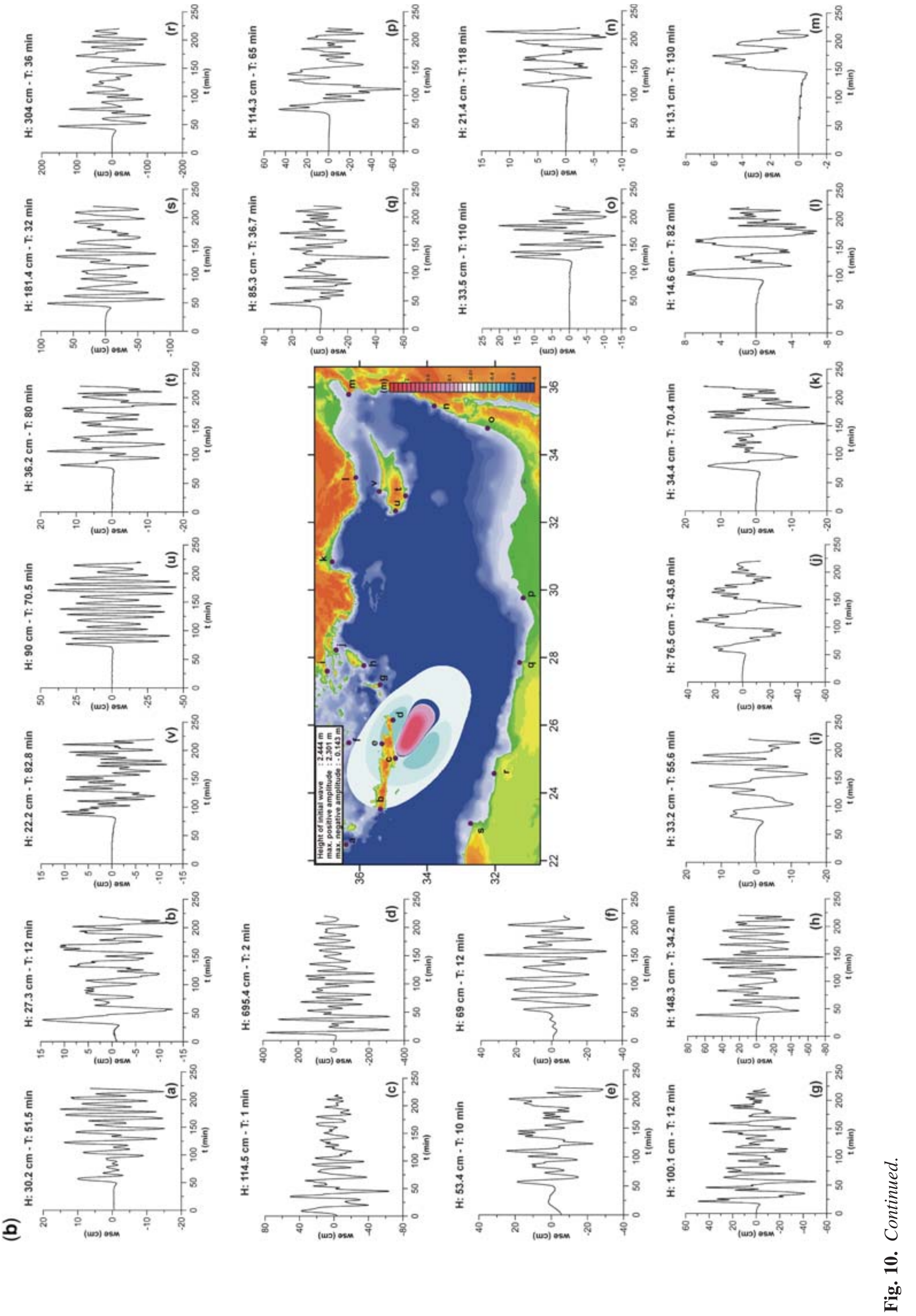

Fig. 10. *Continued.*

after this event tsunami waves were reported to be seen as far as the coastlines of Crete, the Pelepon-nese, Rhodes, Antalya (SW Turkey), Cyprus, Acre and Alexandria–Nile delta (Egypt). In addition, this earthquake and associated damage distributions are listed in most descriptive and parametric catalogues for the Mediterranean basin. However, the orientations of active faults vary along the concave part of the Hellenic arc (e.g. Pliny and Strabo trenches) in accordance with subduction of remnants of old lithospheric slab (Taymaz *et al.* 1990, 1991). Hence, the Hellenic trench in the vicinity of Crete should be considered to be a seismogenic zone of considerable importance in the Mediterranean region (Guidoboni & Comastri 1997).

Figure 9 shows seismic activity of the Hellenic arc and surroundings. The rectangular box with a star indicates the approximate location of the 8 August 1303 Crete earthquake (M $\sim$ 8.0) and tsunami for which simulations are generated by applying an analogous representative earthquake derived from teleseismic P- and SH-wave modelling studies of current earthquakes during instrumental seismology (Taymaz *et al.* 1990; Yolsal & Taymaz 2004, 2005). A snapshot of the initial tsunami waves generated with the parameters given in Figure 9a is shown in Figure 9b. Letters and numbers refer to geographical locations where macroseismic observations were partly reported (Guidoboni & Comastri 2005*a*), and synthetic tsunami mareograms generated at pseudo tide-gauge locations, respectively, and details are displayed in Figure 10. The effects of tsunami waves are clearly visible when synthetic tsunami mareograms at 30, 40, 50, 60, 70 and 80 min are compared (Fig. 10a). The largest wave amplitudes are calculated at the eastern part of Crete (*c*. 7 m at location d). In contrast, the effects of coastal bathymetry and nearshore topography are obvious along the northern African coastline near Alexandria (Egypt), where the maximum wave height is *c*. 1.15 m, whereas at location *q* it is *c*. 85 cm (Fig. 10b). A further clear feature is the extent of the Nile Delta deposits on the Herodotus abyssal plain, which is a NE–SW-trending elongated depression zone bounded by the *c*. 3000 m isobath lying seaward of the northwestern part of the Nile cone; the basin plain stratigraphy consists of thick turbidite muds with pelagic interbeds (see Rothwell *et al.* 2000, figs 3 and 9b). We have synthetically generated many tsunami simulations with different source orientations and displacements, and have been satisfied with a maximum displacement of 8 m ($D_{\max}$), which is in agreement with many historical reports (Ambraseys *et al.* 1994; Guidoboni & Comastri 1997; Hamouda 2006). We consider that this is not too high given the magnitude of reported intensities and macroseismic observations (M $\sim$ 8.0). On the other hand, a maximum displacement of 5 m does not adequately explain the lack (or the excess) of tsunami wave heights at most of the northern Africa coastal plains, including Alexandria and Gaza. This also indicates the importance of source parameters, maximum displacement and of the coastal topography acting as a natural barrier to slow down tsunami sea-waves. It can also be argued that the geometry of the Hellenic arc and of the Pliny–Strabo trenches is responsible for the 1303 tsunamigenic earthquake. This is a rather difficult question to answer, but analogy with current seismicity and source rupture studies implies that a north- to NE-dipping plane with a significant amount of strike-slip component mechanism would better fit the regional and local seismotectonic and geodynamics setting (Taymaz *et al.* 1990; Yolsal & Taymaz 2004, 2005). Of course this is a still open question, but we should keep in mind that there is a dispute about the size and location of the 1303 earthquake in reported historical catalogues. Thus, in the present study we have adopted the best suited location in our simulation study (Fig. 9; Guidoboni & Comastri 1997, 2005*a*). Nevertheless, there are several tsunamis reported to have been caused by strong earthquakes in the vicinity of Rhodes to the east or NE of the island (Papadopoulos *et al.* 2007; Table A3). In contrast, there were other large earthquakes, on 26 June 1926 (M $\sim$ 7.5–8.0) and 25 April 1957 (M $\sim$ 7.2), near Rhodes that did not generate tsunamis; these are, of course, important for tsunami hazard assessment. Thus the question remains: why are some Rhodes earthquakes tsunamigenic and some others not?

Remote sensing and GIS contribution to tsunami risk detection

LANDSAT ETM and digital elevation model (DEM) data derived by the Shuttle Radar Topography Mission (SRTM) provide an excellent opportunity to detect traces of historical tsunami events. On a regional scale the areas of potential tsunami risk are determined by an integration of remote sensing, geological, seismotectonic and topographic data, and historical reports. Furthermore, remote sensing and geographical information system (GIS) methods have proven their utility for the detection of morphological traces of potential ancient tsunami flooding, and in some cases morphological traces of sea-waves as curvilinear scarps open to the sea side are clearly visible (Theilen-Willige 2006). Geomorphometric parameters (i.e. slope degree, minimum or maximum curvatures) provide information on the terrain morphology indicating geomorphological features that might be related to tsunami events. In addition, LANDSAT ETM data are also helpful for deriving information on near-surface water currents in coastal areas that might be useful to improve our understanding of the influence of coastal morphology on the streaming mechanism, which is of great importance for tsunami wave simulation. During the evaluation of the various remote sensing data it has become evident that slope failure caused by undercutting of slope profiles by flood waves is a widespread phenomenon in coastal areas of Eastern Mediterranean countries. One of the procedures to generate a tsunami hazard map could be a comparison between the morphological setting of regions historically affected by major tsunamis and of those affected by recent ones (e.g. the Sumatra earthquake and tsunami of 26 December 2004; Barber *et al.* 2005) and potential risk sites on the Eastern Mediterranean coasts. There are typical features observed in regions prone to catastrophic tsunami events, such as fan-shaped flat areas, drainage patterns, arc-shaped walls and scarps, to name a few. On the other hand, the remnants of tsunami floods can be summarized as irregular swamps, ponds and lagoons near the coast. The details of these issues will be discussed elsewhere.

Implications

There are about a dozen or so strong tsunami events in the Eastern Mediterranean, which reflects an apparent recurrence interval of about 150–200 years (Tables A1–A3), and they are associated mainly either with seismogenic zones of the Hellenic arc, the Gulf of Corinth, central Greece, Sea of Marmara, SW Black Sea, SW Cyprus, the Dead Sea fault and Levantine basin, or with the active volcanic complex of Thera (Santorini, Columbos) and seamounts of the Eastern Mediterranean Sea (Fig. 2). On the other hand, some of the damaging historical tsunamis (e.g. those of 1303 and 1481) in the eastern Hellenic arc also threatened the coastal plains of the Cyprus–Levantine and the Nile Delta regions, as confirmed by our simulations, and thus special care should be taken in the tsunami risk assessment of the region. In this study, numerical tsunami simulations with representative simple source models are presented to examine the probable effects of tsunamis originating in the Hellenic and Cyprus arcs. The likelihood of occurrence of such earthquakes and associated tsunamis is relatively low, but theoretical arrival times (i.e. computed travel times) and water surface elevation (wse) distributions are useful to evaluate the tsunami hazard in the region. In addition, it is obvious for us that tsunami simulations present only rough estimates of expected damage. However, it is essential systematically to conduct field and sedimentological studies to refine flooding estimates for historical and recent tsunamis, as discussed by Dominey-Howes *et al.* (2000). It is also vital to make use of remote sensing technologies embedded in a GIS information database as a complementary tool to existing tsunami hazard studies, to offer an independent approach and to provide a base for further field research. Furthermore, it is important to note that high-resolution bathymetry maps are a crucial component in tsunami wave simulations, and this aspect is rather poorly developed in the Eastern Mediterranean. Thus, future oceanographic and marine geophysical research should aim to improve the resolution of bathymetric maps, particularly for the details of the continental shelf and seamounts.

We thank Istanbul Technical University Research Fund (ITU-BAP), the Turkish National Scientific and Technological Foundation (TÜBİTAK-ÇAYDAG), the Turkish Academy of Sciences (TÜBA) in the framework for Young Scientist Award Program (TT-TÜBA-GEBİP/2001-2-17), and Alexander von Humboldt (AvH) Stiftung for financial support. We are also grateful to P. Wessel and W. H. F. Smith of Hawaii University–NOAA for providing GMT software (Wessel & Smith 1991, 1995). The authors thank N. Shuto, F. Imamura, E. Pelinovsky and A. Kurkin for their invaluable efforts and support for developments of the numerical codes TUNAMI-N2, AVI-NAMI and NAMI-DANCE.

Appendix A

In this Appendix historical tsunamis are summarized in Tables A1–A3 after reliable sources, and relevant references are provided for further sources of observations. UT, Universal Time; *I*, macroseismic intensity; Io, epicentral intensity; Me, equivalent magnitude value (calculated using the method of Gasperini *et al.* (1999) and Gasperini & Ferrari (2000).

Table A1. *Reported tsunamis during the 11th–15th centuries in the Eastern Mediterranean region (compiled after Guidoboni & Comastri 2005*a)

No.	Date	Region of destruction	Geomorphological observations
1	5 December 1033	Israeli–Palestinian (at night; 32°00′N, 35°12′E; Io = IX, Me = 6.0)	Tsunami and subsidence
	There was serious and widespread damage at Jerusalem: part of the city walls and some churches and convents were damaged, as well as the prayer niche (*mihrab*) in the mosque. This earthquake was felt from Egypt to the Negev desert, and from the mountains of Galilee to Syria in the north. The earthquake also had substantial environmental effects: the sources record a tsunami on the coast of Palestine, causing the water in the port of Acre to recede. Evidence of tsunami effects is confined to Acre, because it was a city able to produce written evidence, but it is reasonable to suppose that the tsunami affected the whole coast (Ergin *et al.* 1967; Taher 1979; Soloviev *et al.* 2000).		
2	12 March 1036 or 11 March 1037	Cilicia?–southern Turkey	Tsunami and landslides
	This earthquake is unknown to the seismic catalogue tradition. There is no record of damage, but the earthquake had substantial effects on the environment: mountains were severely shaken, and there were probably some landslides. It has also been reported that there was a strong tsunami in relation to this earthquake (Canard & Berberian 1973).		
3	18 March 1068	Aila (Elat), Israel (06:30 UT; 29° 33′N, 34°57′E; Io = IX, Me = 8.1)	Fissures, formation of new springs
4	29 May 1068	Ramla, Jerusalem (32°34′N, 35°17′E; Io = IX, Me = 6.0)	Tsunami, Euphrates overflowed
	This earthquake is to be located in the sparsely inhabited region between Aila and Taima, and caused environmental effects as the sea withdrew from the Mediterranean coast of Palestine, and then flowed back, engulfing many people. The River Euphrates overflowed its banks (Taher 1979; Ambraseys *et al.* 1994; Soloviev *et al.* 2000).		
5	20 May 1202	Western Syria–Lebanon (02:40 UT; 33°26′N, 35°43′E; Io = X, Me = 7.6)	Tsunami and landslides
	This is one of the strongest and the best documented seismic events in the Mediterranean area, the most advanced historical and seismological study of which has been provided by Ambraseys & Melville (1988). Gigantic waves rose up in the sea between Cyprus and the coast of Syria. The sea withdrew from the coast, ships were hurled onto the eastern coast of Cyprus, fish were thrown onto the shore, and lighthouses were severely damaged (Guidoboni & Traina 1996; Ambraseys & Jackson 1998; Ellenblum *et al.* 1998).		
6	11 May 1222	Cyprus (06:15 UT; 34°42′N, 32°48′E; Io = IX, Me = 6.0)	Tsunami, springs and lake formation
	The towns of Limasol and Nicosia were affected, and especially Paphos, where the castle collapsed and there were many victims. The earthquake was also felt in Egypt. Limasol and Paphos, which are situated on the south and west coast of the island, respectively, were struck by a strong tsunami. The harbour at Paphos was left completely without water (Ergin *et al.* 1967; Ambraseys *et al.* 1994).		

7	8 August 1303	Crete (Greece) (03:30 UT; 35°11′N, 25°38′E; Io = X, Me = 8.0)	Tsunami, landslides, flooding
	This earthquake was one of the largest events in the Mediterranean area, and is referred to in the seismological tradition. There was an enormous reported tsunami that struck Crete, the coast of Egypt and part of Palestine, and less serious effects were observed in the Adriatic (Ambraseys 1962; Taher 1979; Guidoboni & Comastri 1997; El-Sayed *et al.* 2000; Soloviev *et al.* 2000).		
8	18 October 1343	Sea of Marmara (Turkey) (16:15 UT; 41°03′N, 29°04′E; I = VIII)	Tsunami
	A large sea wave penetrated a long stretch of lowlying coast to a distance of about 1.8 km. Some boats were dragged from ports or other coastal places where they were lying, and left behind. After a considerable time, the sea receded, leaving mud and dead fish on land (Ergin *et al.* 1967; Taher 1979; Papazachos & Papazachou 1997; Soloviev *et al.* 2000; Ambraseys 2002*a*,*b*; Guidoboni & Comastri 2002).		
9	20 March 1389	Chios (Greece) (12:30 UT; 38°16′N, 26°31′E; Io = VIII–IX, Me = 5.8)	Tsunami
	A sea-wave penetrated as far as the market square in Chios. Those present fled in fright to a nearby hill (Ambraseys 1962; Ergin *et al.* 1967; Papazachos & Papazachou 1997; Soloviev *et al.* 2000).		
10	July 1402	Gulf of Corinth (Greece) (38°09′N, 22°20′E; Io = X, Me = 6.3)	Tsunami, landslides, fissures
	The earthquake was accompanied by a strong tsunami that struck both shores of the Gulf of Corinth. The tsunami was more violent on the northern shore: first the sea drew back about 970 m from the coast, and then it flowed back over the shore, penetrating more than 200 m, destroying the wheat crop. There was an increased flow of water from springs at Patras and Corinth (Ambraseys 1962; Ergin *et al.* 1967; Ambraseys & Melville 1995; Soloviev *et al.* 2000).		
11	29 December 1408	Western Syria and Cyprus (35°40′N, 36°10′E; Io = IX, Me = 6.0)	Tsunami, landslides, avalanches
	The earthquake was accompanied by a tsunami, perhaps in the stretch of a sea opposite or to the south of Mt. Cassius, but there is no specific information available about its location. However, it has been suggested that the ‘surface-faulting’ may have stretched for at least 20 km from Qusayr, either SW towards the coast, or southwards along one or more strands of the Dead Sea fault. The tsunami threw boats out of the sea onto the shore, but there was no other damage (Taher 1979; Ambraseys & Melville 1995; Ambraseys & Jackson 1998).		
12	19 December 1419 or 16 January 1420	İstanbul, NW Turkey	Tsunami?
	The earthquake was a damaging one, and there was probably a tsunami as well, although the sources simply refer to unusual tides (Taher 1979; Papazachos & Papazachou 1997; Ambraseys 2002*b*).		
13	3 May 1481 and 17–18–19 December 1481	Southern Aegean, Rhodes, Antalya	Tsunami

(*Continued*)

Table A1. Continued

No.	Date	Region of destruction	Geomorphological observations
	3 May 1481	06:30 UT:	Rhodes, 36°26′N, 28°13′E; I = V–VI
			Antalya, 36°53′N, 30°42′E
	3 October 1481		Rhodes, 36°26′N, 28°13′E; I = V–VI
	17 December 1481	22:00 UT:	Rhodes, 36°26′N, 28°13′E; I = V–VI
	18 December 1481	03:00 UT:	Rhodes, 36°26′N, 28°13′E; I = V–VI
	18 December 1481	05:15 UT:	Rhodes, 36°26′N, 28°13′E; I = VIII–IX
	19 December 1481	05:15 UT:	Rhodes, 36°26′N, 28°13′E; I = IV–V
	This earthquake series was very violent with many aftershocks, but did not cause extensive damage. However, the town of Rhodes was flooded by a tsunami that reached a height of about 3 m. Immediately afterwards, the sea flowed back and returned to its normal level. Some collapses were reported (Ambraseys 1962; Ben-Menahem 1979; Papazachos *et al.* 1986; Soloviev *et al.* 2000).		
14	1 July 1494	Crete (Greece) (10:10 UT; 35°12′N, 24°55′E; Io = VIII–IX)	Tsunami
	This earthquake was strong enough to create a local tsunami at Candia harbour. All the ships at anchor struck violently against each other to the extent that they seemed likely to break up (Ambraseys 1962; Soloviev *et al.* 2000).		

Table A2. *Reported tsunamis in the Levantine basin and surrounding regions from 1365 BC to AD 1900 (compiled after Sbeinati* et al. 2005)

No.	Date and magnitude	Observed intensity locations	Geomorphological observations	References
1	*c*. 1365 BC	VIII–IX (Ugharit) VII (Tyre)	Tsunami and fire	S48, S82, BM79
2	590 BC (M_L 6.8)	VII (Tyre)	Tsunami (Tyre and Lebanese coast)	BM79, PK81, S32
3	525 BC (M_L 7.5)	VIII–IX (Tyre, Sidon) III–IV (Cyclades and Euboea islands)	Tsunami (Bisri and Lebanese coast)	S32, BM79, PK81
4	148–130 BC	VII (Antioch)	Tsunami (Syrian coast)	S32, G94
5	92 BC (M_L 7.1)	III–IV (Syria, Egypt)	Tsunami (Levantine coast)	BM79, PK81
6	13 December 115 (M_L 7.4)	VII (Antioch) VI–VII (Mirana) V (Rhodes), Pitana	Tsunami (Antioch, Yavne, Caesaria, Palestine)	BM79, PK81
7	303–304 (M_L 7.1)	VIII (Sidon, Tyre) VII (Syria) III–IV (Al-Quds)	Tsunami (Caesaria in Palestine)	BM79, PK81, G94
8	348–349 (M_L 7.0)	VII (Beirut) VI (Arwad)	Tsunami (Beirut, Arwad)	S32, BM79, G94
9	9 July 551	IX–X (Beirut, Sur, Tripoli, Byblus, Al-Batron) VII–VIII (Sarfand, Sidon) III–IV (Arwad)	Tsunami (Lebanese coast) Landslide (near Al-Batron)	S32, PK81, D00
10	18 January 749	VII–IX (Mount Tabor) VIII (Baalbak, Nawa, Balqa) VII (Basra, Al-Quds, Tabaryya, Al-Ghouta, Manbej) VII–VIII (Beit Qubayeh) VI (Daraya) V–VI (Ariha)	Tsunami, liquefaction, landslides and surface faulting	BM79, R85, G94
11	5 April 991 (M_L 6.5)	VIII–IX (Baalbak) VII–VIII (Damascus) III–IV (Egypt)	Tsunami (Syria)	S32, G94

(*Continued*)

Table A2. Continued

No.	Date and magnitude	Observed intensity locations	Geomorphological observations	References
12	November 1114 (M_L 7.0)	VIII (Maskaneh) VII–VIII (Maraş, Samsat, Urfa) VII (Harran) V (Aleppo) IV (Antioch)	Tsunami (in Palestine) and landslides	BM79, PK81
13	29 June 1170 (M_L 7.9)	VII–VIII Damascus, Homs, Hama, Al-Sham, Lattakia, Baalbak, Shaizar) VII (Barin) VII–VIII (Aleppo) V (Iraq, Al Jazira, Al-Mousel)	Tsunami	AB89, PK81
14	20 May 1202	IX (Mount Lebanon, Baalbak, Tyre, Beit Jin) VIII (Nablus, Banyas, Al-Samyra, Damascus, Hauran, Hama, Tripoli)	Tsunami, landslides and aftershocks	AM88, A94, Table A1
15	8 August 1303	VII (Cairo, Alexandria, Damanhur, Safad) VI (Damascus, Hama) IV (Antioch, Tunus, Barqa, Morocco, Cyprus, Istanbul, Sicily)	Tsunami (Alexandria, Cairo-Damascus)	PK81, Table A1
16	20 February 1404	VI–VII (Qalaat) VIII (Bkas) VII–VIII (West of Aleppo, Qalaat Al-Marqeb) VII (Tripoli, Lattakia, Jableh)	Tsunami (Aleppo)	S32, AB89, AM95
17	29 December 1408	VIII–IX (Shugr, Bkas) VIII (Blatnes) VII (Lattakia, Jableh, Antioch) VI (Syria)	Tsunami	PT80, AM95, Table A1
18	29 September 1546	VI–VII (Nablus) V (Damascus) VI (Al-Quds, Yafa, Tripoli) V (Famagusta)	Tsunami	S32, PK81
19	21 July 1752 (M_L 7.0)	VII (Lattakia) V (Tripoli)	Tsunami (Syrian coast)	S32, BM79

20	30 October 1759 (M_L 6.5)	VIII (Al-Qunaytra) VII (Safad) VI (Acre, An-Nasra, Sidon, Saasaa) V (Damascus) IV (Aleppo, Al-Quds, Beirut, Antioch, Gaza, Cyprus)	Tsunami (Acre and Tripoli)	S32, BM79, AM89
21	25 November 1759 (M_L 6.8)	$>$VIII (Baalbak, Serghaya, Zabadani) VII (Ras Baalbak, Al-Qunaytra) VII–VIII (Damascus, Beirut, Sidon, Safad, Sur) VII (Tripoli, Acre) VI–VII (Homs, Hama, An-Nasra, Hosn Al-Akrad) V–VI (Lattakia, Al-Quds, Gaza)	Tsunami and faulting	BM79, AB89
22	13 August 1822 (M_L 7.1; M_S 7.4)	IX (Jisr Ash Shoughour, Quseir) VIII–IX (Aleppo, Darkoush) VIII (Antioch, Iskenderun, Idleb, Sarmeen, Kelless) VII–VIII (Armanaz, Sarmada) VII (Lattakia, Homs, Hama, Maraş, Ram Hamadan, Bennesh, Maarret Missrin) III (Damascus, Gaza, Al-Quds, Black Sea, Cyprus)	Tsunami and faulting (İskenderun, Beirut, Cyprus, Jerusalem)	BM79, PT80, A89
23	1 January 1837 (M_L 6.4)	VII–VIII (Safad, Nablus, Beit Lahm, Al-Khali) VII (Tabariya) VI–VII (Beirut) VI (Damascus)	Tsunami	S32, BM79
24	3 April 1872 (M_L 7.3; M_S 7.2)	VIII (Harem, Armanaz) VII–VIII (Buhyret Al-Amq, Antioch) VII (Aleppo, Suaidiya) VI–VII (Izaz, Idleb, Iskenderun) IV (Hama, Homs, Tripoli) III (Damascus, Beirut, Sidon, Diyarbakır, Egypt, Rhodes)	Tsunami	A89, AB89, PT80

References: A89, Ambraseys 1989; AB89, Ambraseys & Barazangi 1989; AF95, Ambraseys & Finkel 1995; AF93, Ambraseys & Finkel 1993; AM88, Ambraseys & Melville 1988; AM95, Ambraseys & Melville 1995; A94, Ambraseys *et al.* 1994; BM79, Ben-Menahem 1979; D00, Darawcheh *et al.* 2000; E67, Ergin *et al.* 1967; G94, Guidoboni *et al.* 1994; PK81, Plassard & Kogoj 1981; PT80, Poirier & Taher 1980; R85, Russel 1985; S82, Saadeh 1982; S05, Sbeinati *et al.* 2005; S48, Schaeffer 1948; S32, Sieberg 1932; M_L, local magnitude.

Table A3. *Reported tsunamis along the Hellenic arc and trench system (compiled after Papadopoulos* et al. *(2007) and Papadopoulos & Fokaefs (2005)*

No.	Date	Geographical region, Intensity, magnitude	Geomorphological observations
1	(222?) 227 BC	Rhodes, Tilos, Carian and Lycian towns (36°30′N, 27°48′E; Io: IX; Ms: 7.5)	Sea wave in Rhodes
	Sieberg (1932) stated that a seismic sea wave was associated with the earthquake but this is not justified by the available historical documentation Ambraseys 1962; Papadopoulos 2001).		
2	66	South of Crete (35°12′N, 23°30′E)	Crete
3	148	Rhodes, Dodecanese Islands (36°18′N, 28°36′E; Io: IX; Ms: 7.0)	Destructive sea inundation
	In the rhetorical speech 'Rodiakos' of Aristides Aelius (AD129–189), to the citizens of Rhodes, a strong tsunami caused by the earthquake is described (see passages 20–26): 'and I remember that in that fatal noon, when the calamity that happened to you started, when the sea was calm, . . . and all the earthquake force was directed against the city. . . Then the sea water retreated and the ports dried up. . . And the ports became as the dry ground. . . And everything happened at the same moment: the earthquake of the sea, the clouds of the roaring, the lamentations, the noise of the dead bodies, the ground subsidence. . . Everything had collapsed'. (Papadopoulos *et al.* 2007).		
4	262	South Asia Minor (36°30′N, 27°48′E)	Sea inundation
	Although there were a number of serious disasters in several parts of the Mediterranean, namely at Rome, and in Libya and Asia Minor (Ambraseys 1962; Antonopoulos 1980; Guidoboni *et al.* 1994), documents concerning earthquakes and associated sea disturbances remain rather uncertain.		
5	21 July 365	Crete (36°N, 23°E)	Crete
6	(554?) 556	Cos, Dodecanese islands (36°48′N, 27°18′E; Io: 10; Ms: 7.0)	Destructive earthquake and tsunami
	Agathias (536–582) reported that the island of Cos 'was shaken and only a very small part of it saved, while the rest collapsed . . . The sea rose up greatly and inundated the buildings along the coast and caused destruction to human beings and their property.' The exact date of the earthquake remains uncertain.		
7	8 August 1303	Crete and Dodecanese Islands (35°00′N, 27°00′E; Io: X; Ms: 8.0)	Destructive inundation
	According to many historical records (Ambraseys 1962; Ambraseys *et al.* 1994; Guidoboni & Comastri 1997), this earthquake was a very large tsunamigenic earthquake that occurred in the eastern segment of the Hellenic arc between Crete and Rhodes. It created a strong tsunami wave that affected Crete, Acre, Alexandria and Rhodes. Historical records indicated that the sea swept into Crete with such a force that it destroyed buildings and killed inhabitants; also, the Nile was flooded with great sound, throwing boats a bow-shot on land and smashing their anchors; then the water retreated leaving the boats on land (Antonopoulos 1980; El-Sayed *et al.* 2000; Papadopoulos *et al.* 2007). However, Evagelatou-Notara (1993) and Guidoboni & Comastri, (1997) did not support that Rhodes was damaged by this tsunami, and considered that three sediment layers found in Dalaman, SW Turkey, could be attributed to the 1303 tsunami (Papadopoulos *et al.* 2004). (See also Tables A1 and A2.)		

8	03 May 1481	Rhodes (at night; 36°30′N, 28°20′E; Io: VII; Ms: 6.5)	Damaging wave in Rhodes
	This earthquake caused a 3 m high tsunami that flooded the coast, and a ship that was moved ashore was smashed in a reef and sank with all its crew (Coronelli & Parisotti 1688; Tables A1 and A2). Ben-Menahem (1979) reported a tsunami as far away as the Levantine coasts, and Papadopoulos *et al.* (2004) suggested that radiocarbon dating of the medium tsunami sediment layer found at Dalaman indicates deposition in AD 1473 $\pm$ 46.		
9	1489	Dodecanese Islands, Antalya (36°36′N, 28°24′E)	Strong withdrawal
	This earthquake is questionable; a tsunami was described by Leonardo da Vinci to have occurred in 1489: ‘In (fourteen hundred) and 89 there was an earthquake in the sea of Adalia (Antalya, south of Anatolia) near Rhodes, which opened the (floor of the) sea, and into this opening such a torrent water poured that for more than three hours the floor of the sea was uncovered by the reason of the water which was lost in it, and then it closed (the sea coming) its former level’ (Baratta 1903; Ambraseys 1962; Antonopoulos 1980).		
10	1 July 1494	Crete	Tsunami
	See Tables A1 and A2 for details.		
11	April 1609	Rhodes, SE Aegean Sea (36°24′N, 28°20′E; Io: IX; Ms: 7.2)	Sea-waves in Rhodes, Dalaman
	This earthquake was very large and caused tsunami waves affecting Rhodes and the Eastern Mediterranean coasts. Ambraseys & Finkel (1995) compiled the historical catalogues and showed that: ‘half of the town, including the castle, was ruined, and (an exaggerated figure of) over 10 000 people were reported drowned by a sea-wave… This appears to have been a great earthquake, felt also in various places in Egypt and the Syrian coast but further details are lacking.’ Papadopoulos *et al.* (2004) did not find the 1609 tsunami in the Dalaman sedimentary stratigraphy.		
12	8 November 1612	North coasts of Crete (35°30′N, 25°12′E; Io: VIII; Ms: 7.0)	Damaging inundation
13	9 March 1630	Kythira, SE Aegean Sea	Tsunami
14	14 February 1672	North Aegean Sea, Cos (39°42′N, 26°00′E; Io: VIII; Ms: 6.8)	Sea-waves in Cos
	This strong earthquake was felt not only in Lesvos and Tenedos, and then NE Aegean Sea, but also as far away as Cos, in the SE Aegean Sea, where a sea wave is said to have followed the shock (Sieberg 1932; Montandon 1953; Ambraseys & Finkel 1995; Papadopoulos 2001; Papadopoulos *et al.* 2007).		
15	31 January 1741	Rhodes, SE Aegean Sea (to: UT01 (Universal Time) 15; 36°12′N, 28°30′E; Io: VIII; Ms: 7.3)	Very strong waves in Rhodes

(*Continued*)

Table A3. Continued

No.	Date	Geographical region, Intensity, magnitude	Geomorphological observations
	This large, destructive and tsunamigenic event occurred between Rhodes and Cyprus, where minarets fell and the church of Santa Sophia in Famagusta was damaged (Ambraseys *et al.* 1994). According to historical document (Ambraseys & Finkel 1995): 'As a result of the earthquake, the sea in Rhodes retreated and then flooded the coast 12 times with great violence, submerging the coast opposite the island and destroying five or six villages located a kilometre inland'. Also, the upper tsunami sediment layer discovered in Dalaman by Papadopoulos *et al.* (2004) could be attributed to the 1741 tsunami.		
16	14 March 1743	Antalya	Sea withdrawal
	Ambraseys & Finkel (1995) reviewed a report from Cyprus indicating the strong destructive earthquakes that shook the Antalya area to the east of Rhodes. In this report: 'I have been informed from Satalia (Antalya) that from the 8th to 20th of the month there were terrible earthquakes as a result of which the port dried up for some time, many houses collapsed as well as part of the walls at different places which fell on the consul's house, destroying it. Many villages were lost in these earthquakes and a mountain opposite that, which lies west of the islet of Rachat, sunk completely'.		
17	28 February 1851	South Asia Minor, Fethiye, Mugla, Rhodes (36°24′N, 28°42′E; Io: IX; Ms: 7.1)	Sea-wave in Fethiye
	Many historical documents indicate that this event was very strong and it caused destruction in Fethiye, SW Turkey and in Rhodes (Ambraseys 1962; Ambraseys *et al.* 1994; Papazachos & Papazachou 1997). It is supported that the coast was flooded about 0.6 m above the normal sea-water level at Fethiye (Perrey 1855; Ambraseys 1962; Antonopoulos 1980).		
18	3 April 1851	South Asia Minor, Fethiye Gulf (36°24′N, 28°42′E)	Sea-waves in Fethiye
	The tsunami intensity is proposed as three, and this event was possibly an aftershock of the 28 February 1851 earthquake (Ambraseys *et al.* 1994). Historical documents indicated about 1.8 m high inundation (height of the tsunami wave) in Fethiye region.		
19	23 May 1851	Rhodes, Dodecanese Islands (36°24′N, 28°42′E)	Sea-waves in Rhodes
	This was another aftershock of the 28 February 1851 earthquake, and reported inundation by tsunami waves in Rhodes and Chalki is doubtful.		

20	13 February 1855	South Asia Minor, Fethiye Gulf	Sea-waves in Fethiye
	Doubtful inundation in Fethiye was reported by Schmidt (1879) and Perrey (1855) for this earthquake.		
21	30 August 1926	Argolikos Gulf, SW Aegean Sea ($36^\circ 30'$N, $23^\circ 18'$E)	Tsunami
22	9 February 1948	Karpathos, SE Aegean Sea (to UT 12:58:13; $35^\circ 30'$N, $27^\circ 12'$E; Io: IX; Ms: 7.1)	Damaging sea-waves in Karpathos
	As reported by Galanopoulos (1955, 1960), destruction was caused near Pigadia, Karpathos and ‘a huge seismic sea-wave that penetrated inland 1 km’; the first motion of the sea was withdrawal (Papadopoulos *et al.* 2007). A few eyewitnesses reported that the first tsunami wave arrived about 5–10 min after the earthquake and many vessels were moved ashore and destroyed. Field surveys indicated that the wave height was about 2.5 m in Pigadia, penetration inland was about 250 m at its maximum to the west of Pigadia, and time of arrival after the earthquake occurrence ranged between 5 and 10 min (Papadopoulos *et al.* 2007).		
23	9 July 1956	Greek archipelago, South Aegean Sea Amorgos, Astypalea (to UT 03:11:40; $36^\circ 38'$N, $25^\circ 58'$E; Io: IX; Ms: 7.5)	Destructive large wave
	This event is one of the largest and best documented tsunamigenic earthquakes in the Aegean Sea during the 20th century (Stiros *et al.* 1994). It occurred near the SW coast of the island of Amorgos, killing 53 people, injuring 100 and destroying hundreds of houses. Tsunami waves were reported to be particularly high on the SE coast of Amorgos (*c.* 30 m) (Ambraseys 1962) and on the north coast of the island of Astypalaea. It was probably generated by either one or a series of submarine sediment slides down the slopes of the Amorgos–Astypalaea Trough (Perissoratis & Papadopoulos 1999; Dominey-Howes *et al.* 2000). The reported run-up elevations for the tsunami waves varied depending to local bathymetry and coastal configuration (Ambraseys 1962; Antonopoulos 1980; Papazachos *et al.* 1986).		
24	5 April 2000	Heraklion, North Crete	Tsunami
25	24 March 2002	City of Rhodes ($36^\circ 27'$N, $28^\circ 12'$E; Ms: 7.5)	
	Local press reports indicated that sea waves along the coasts of Rhodes reached 3–4 m high and they overtopped an elevated wall, which protects the coastal street from sea-waves, and inundated a coastal segment as long as 2 km. The origin of the tsunami was thought to be aseismic submarine slides, because of the lack of an earthquake before or after the tsunami occurrence in the general region of Rhodes (Papadopoulos *et al.* 2007).		

References

ABE, K. 1979. Size of great earthquakes of 1837–1974 inferred from tsunami data. *Journal of Geophysical Research*, **84**, 1561–1568.

ABE, K. 1981. Physical size of tsunamigenic earthquakes of the northwestern Pacific. *Physics of the Earth and Planetary Interiors*, **27**, 194–205.

ABE, K. 1985. Quantification of major earthquake tsunamis of the Japan Sea. *Physics of the Earth and Planetary Interiors*, **38**, 214–223.

ABE, K. 1989. Quantification of tsunamigenic earthquakes by the Mt scale. *Tectonophysics*, **166**, 27–34.

AMBRASEYS, N. N. 1962. Data for the investigation of the seismic sea-waves in the Eastern Mediterranean. *Bulletin of the Seismological Society of America*, **52**, 895–913.

AMBRASEYS, N. N. 1989. Temporary seismic quiescence: SE Turkey *Geophysical Journal International*, **96**, 311–331.

AMBRASEYS, N. N. 2002*a*. The seismic activity of the Marmara Sea region over the last 2000 years. *Bulletin of the Seismological Society of America*, **92**, 1–18.

AMBRASEYS, N. N. 2002*b*. Seismic sea-waves in the Marmara Sea region during the last 20 centuries. *Journal of Seismology*, **6**, 571–578.

AMBRASEYS, N. N. & BARAZANGI, M. 1989. The 1759 earthquake in the Bekaa Valley: implications for earthquake hazard assessment in the Eastern Mediterranean region *Journal of Geophysical Research*, **94**, 4007–4013.

AMBRASEYS, N. N. & FINKEL, C. F. 1993. Material for the investigation of seismicity of the Eastern Mediterranean region during the period 1690–1710. *In*: STUCCHI, M. (ed.) *Materials of the CEC Project 'Review of Historical Seismicity in Europe'*, 1. CNR, Milan, 173–194.

AMBRASEYS, N. N. & FINKEL, C. F. 1995. *The seismicity of Turkey and adjacent areas: a historical review* (*1500–1800*). Muhittin Salih EREN Publications, İstanbul.

AMBRASEYS, N. N. & JACKSON, J. A. 1998. Faulting associated with historical and recent earthquakes in the eastern Mediterranean region. *Geophysical Journal International*, **133**, 390–406.

AMBRASEYS, N. N. & MELVILLE, C. P. 1988. An analysis of the Eastern Mediterranean Earthquake of 20 May 1202, *In*: LEE, W. H., MEYERS, H. & SHIMAZAKI, K. (eds) *Historical Seismograms and Earthquakes of the World*. Academic Press, San Diego, CA, 181–200.

AMBRASEYS, N. N. & MELVILLE, C. P. 1995. Historical evidence of faulting in eastern Anatolia and northern Syria. *Annali di Geofisica*, **38**, 337–343.

AMBRASEYS, N. N., MELVILLE, C. P. & ADAMS, R. D. 1994. *The Seismicity of Egypt, Arabia and the Red Sea: a Historical Review*. Cambridge University Press, Cambridge.

ANTONOPOULOS, J. 1980. Data from investigation on seismic sea-waves events in the Eastern Mediterranean from the birth of Christ to 1980 AD (6 parts). *Annali di Geofisica*, **33**, 141–248.

BARATTA, M. 1903. Leonardo da Vinci ed i problemi della terra. *Biblioteca Vinciana*, **1**, 292–293.

BARBER, A. J., CROW, M. J. & MILSOM, J. S. (eds) 2005. *Sumatra: Geology, Resources and Tectonic Evolution*. Geological Society, London, Memoirs, **31**.

BEN-MENAHEM, A. 1979. Earthquake catalogue for the Middle East (92 B.C.–1980 A.D.). *Bolletino di Geofisica Teorica ed Applicata*, **21**, 245–310.

BOSCHI, E., TINTI, S., ARMIGLIATO, A. *ET AL*. 2005. A tsunami warning system for the Mediterranean: a utopia that could be implemented in a short time. EGU-2005 General Assembly, NH6.01 Tsunamis. *Geophysical Research Abstracts*, **7**, Sref-ID:1607-7962/gra/EGU05-A-09852.

CANARD, H. & BERBERIAN, M. 1973. *Aristakes de Lastivert. Recit des malheurs de la nation armenienne*. Editions de Byzantion, Brussels.

CORONELLI, P. & PARISOTTI, V. 1688. *Isola di Rodi geografica, storica, antica e moderna*. Venice.

DARAWCHEH, R., SBEINATI, M. R., MARGOTTINI, C. & PAOLINI, S. 2000. The 9 July 551 AD Beirut earthquake, Eastern Mediterranean region. *Journal of Earthquake Engineering*, **4**, 403–414.

DOMINEY-HOWES, D., CUNDY, A. & CROUDACE, I. 2000. High energy marine flood deposits on Astypalaea Island, Greece: possible evidence for the AD 1956 southern Aegean tsunami. *Marine Geology*, **163**, 303–315.

ELLENBLUM, R., MARCO, S., AGNON, A., ROCKWELL, T. & BOAS, A. 1998. Crusader castle torn apart by earthquake at dawn, 20 May 1202. *Geology*, **26**, 303–306.

EL-SAYED, A., ROMANELLI, F. & PANZA, G. 2000. Recent seismicity and realistic waveforms modeling to reduce the ambiguities about the 1303 seismic activity in Egypt. *Tectonophysics*, **328**, 341–357.

ERGIN, K., GÜÇLÜ, U. & UZ, Z. 1967. *A Catalogue of Earthquakes of Turkey and Surrounding Area* (*11 A.D. to 1964 A.D.*). Istanbul Technical University Press, Istanbul.

EVAGELATOU-NOTARA, F. 1993. *Earthquakes in Byzantium from 13th to 15th century—a Historical Examination*, **24**. Parousia, Athens [in Greek with English summary].

FOKAEFS, A. & PAPADOPOULOS, G. A. 2006. Tsunami hazard in the Eastern Mediterranean: strong earthquakes and tsunamis in Cyprus and the Levantine Sea. *Natural Hazard*, doi:10.1007/s11069-006-9011-3.

GALANOPOULOS, A. G. 1955. The seismic geography of Greece. *Annales Géologiques des Pays Helléniques*, **6**, 83–121 [in Greek].

GALANOPOULOS, A. G. 1960. Tsunamis observed on the coasts of Greece from Antiquity to present time. *Annale di Géofisica*, **13**, 369–386.

GASPERINI, P. & FERRARI, G. 2000. Deriving numerical estimates from descriptive information: the computation earthquake parameters. *Annali di Geofisica*, **43**, 729–746.

GASPERINI, P., BERNARDINI, F., VALENSISE, G. & BOSCHI, E. 1999. Defining seismogenic sources from historical felt reports. *Bulletin of the Seismological Society of America*, **89**, 94–110.

GEBCO 1997. *General Bathymetric Chart of the Oceans, Digital Version*. Distributed on CD-ROM by the British Oceanographic Data Centre, Birkenhead.

GOTO, C., OGAWA, Y., SHUTO, N. & IMAMURA, F. 1997. Numerical method of tsunami simulation with the leap-frog scheme (IUGG/IOC Time Project). *IOC Manual, UNESCO*, **35**.

GUIDOBONI, E. & COMASTRI, A. 1997. The large earthquake of 8 August 1303 in Crete: seismic scenario and tsunami in the Mediterranean area. *Journal of Seismology*, **1**, 55–72.

GUIDOBONI, E. & COMASTRI, A. 2002. A 'belated' collapse and a false earthquake in Constantinople: 19 May 1346. *European Earthquake Engineering*, **3**, 22–26.

GUIDOBONI, E. & COMASTRI, A. 2005*a*. *Catalogue of earthquakes and tsunamis in the Mediterranean area from the 11th to the 15th century*. INGV-SGA, Bologna.

GUIDOBONI, E. & COMASTRI, A. 2005*b*. Two thousand years of earthquakes and tsunamis in the Aegean arc (from 5th BC to 15th century). *In*: TAYMAZ, T. (ed.) *International Symposium on the Geodynamics of Eastern Mediterranean: Active Tectonics of the Aegean Region*, 15–18, June 2005, Kadir Has University, İstanbul, Abstracts Volume, p. 242.

GUIDOBONI, E. & TRAINA, G. 1996. Earthquakes in medieval Sicily: a historical revision (7th–13th century). *Annali di Geofisica*, **39**, 1201–1225.

GUIDOBONI, E., COMASTRI, A. & TRAINA, G. 1994. *Catalogue of ancient earthquakes in the Mediterranean area up to the 10th century*. ING-SGA, Bologna.

HAMOUDA, A. Z. 2006. Numerical computations of 1303 tsunamigenic propagation towards Alexandria, Egyptian coast. *Journal of African Earth Sciences*, **44**, 37–44.

LE PICHON, X., LYBERIS, N. & ALVAREZ, F. 1984. Subsidence history of the North Aegean trough. *In*: DIXON, J. E. & ROBERTSON, A. H. F. (eds) *Geological Evolution of the Eastern Mediterranean*. Geological Society, London, Special Publications, **17**, 27–741.

MAKRIS, J. & STOBBE, C. 1984. Physical properties and state of the crust and upper mantle of the eastern Mediterranean Sea deduced from geophysical data. *Marine Geology*, **55**, 347–363.

MCCLUSKY, S., BALASSANIAN, S., BARKA, A. *ET AL.* 2000. Global positioning system constraints on plate kinematics and dynamics in the eastern Mediterranean and Caucasus. *Journal of Geophysical Research*, **105**, 5695–5719.

MCCLUSKY, S., REILINGER, R., MAHMOUD, S., BEN-SARI, D. & TEALEB, A. 2003. GPS constraints on Africa (Nubia) and Arabia plate motions. *Geophysical Journal International*, **155**, 126–138.

MINOURA, K., IMAMURA, F., KURAN, U., NAKAMURA, T., PAPADOPOULOS, G. A., TAKAHASHI, T. & YALÇINER, A. C. 2000. Discovery of Minoan tsunami deposits. *Geology*, **28**, 59–62.

MONTANDON, F. 1953. *Les tremblements de terre destructeurs en Europe, Catalogue par territoires seismique, de l'an 1000 à 1940.* L'Union internationale de Secours, Geneva.

MURTY, T. S. & LOOMIS, H. G. 1980. A new objective tsunami magnitude scale. *Marine Geodesy*, **4**, 267–282.

OKADA, Y. 1985. Surface deformation due to shear and tensile faults in a half-space. *Bulletin of the Seismological Society of America*, **75**, 1135–1154.

OKAL, E. A. 1988. Seismic parameters controlling far-field tsunami amplitudes: a review. *Natural Hazards*, **1**, 67–96.

PAPADOPOULOS, G. A. 2001. Tsunamis in the East Mediterranean: a catalogue for the area of Greece and adjacent seas. *In*: *Proceedings of Joint IOC–IUGG International Workshop, 'Tsunami Risk Assesment beyond 2000: Theory, Practice and Plans'*, 14–16 June 2000, Moscow, 34–43.

PAPADOPOULOS, G. A. & FOKAEFS, A. 2005. Strong tsunamis in the Mediterranean Sea: a re-evaluation. *ISET Journal of Earthquake Technology*, **42**, 159–170.

PAPADOPOULOS, G. A. & SATAKE, K. (eds) 2005. *Proceedings of the 22nd IUGG International Tsunami Symposium*, 27–29, June 2005. IUGG-UGGI, Chaina, Crete, Greece.

PAPADOPOULOS, G. A., IMAMURA, F., MINOURA, K., TAKAHASI, T., KURAN, U. & YALÇINER, A. C. 2004. Strong earthquakes and tsunamis in the East Hellenic Arc. *European Geosciences Union—Geophysical Research Abstracts*, **6**, 03212.

PAPADOPOULOS, G. A., DASKALAKI, E., FOKAEFS, A. & GIRALEAS, N. 2007. Tsunami hazard in the Eastern Mediterranean: strong earthquakes and tsunamis in the east Hellenic Arc and Trench system. *Natural Hazards and Earth System Sciences*, **7**, 57–64.

PAPAZACHOS, B. C. & PAPAZACHOU, C. 1997. *The Earthquakes of Greece*. Ziti Publications, Thessaloniki.

PAPAZACHOS, B. C., KOUTITAS, CH., HATZIDIMITRIOU, P. M. & PAPAIOANNOU, CH. A. 1986. Tsunami hazard in Greece and the surrounding area. *Annali di Geofisica*, **4B**, 79–90.

PAPAZACHOS, B. C., PAPADIMITRIOU, E. E., KIRATZI, A. A., PAPAZACHOS, C. B. & LOUVARI, E. K. 1998. Fault plane solutions in the Aegean Sea and the surrounding area and their implication. *Bollettino di Geofisica Teorica ed Applicata*, **39**, 199–218.

PAPAZACHOS, B. C., PAPAIOANNOU, C. A., PAPAZACHOS, C. B. & SAVVAIDIS, A. S. 1999. Rupture zones in the Aegean region. *Tectonophysics*, **308**, 205–221.

PELINOVSKY, E., KHARIF, C., RIABOV, I. & FRANCIUS, M. 2001. Study of tsunami propagation in the Ligurian Sea. *Natural Hazards and Earth System Sciences*, **1**, 195–201.

PERISSORATIS, C. & PAPADOPOULOS, G. C. B. 1999. Sediment instability and slumping in the southern Aegean Sea and the case history of the 1956 tsunami. *Marine Geology*, **161**, 287–305.

PERREY, A. 1855. Note sur les tremblements de terre en 1584, avec supplements pour les années antérieures 1852–1853. *Bulletin of the Royal Academy of Sciences, Brussels*, **22-I**, 526–572.

PLASSARD, J. & KOGOJ, B. 1981. *Seismicité du Liban: catalogue des seismes ressentis*, 3rd edn. Collection des Annales-Mémoires de l'Observatoire de Ksara, IV, Beirut.

POIRIER, J. & TAHER, M. 1980. Historical seismicity in the Near and Middle East, North Africa, and Spain from Arabic documents (VII–XVIIIth century). *Bulletin of the Seismological Society of America*, **70**, 2185–2201.

ROTHWELL, R. G., REEDER, M. S., ANASTASAKIS, G., STOW, D. A. V., THOMSON, J. & KAHLER, G. 2000. Low sea-level stand emplacement of megaturbidites in the western and eastern Mediterranean Sea. *Sedimentary Geology*, **135**, 75–88.

RUSSEL, K. W. 1985. The earthquake chronology of Palestine and northwest Arabia from the 2nd through the mid-8th century A.D. *Bulletin of the American School of Oriental Research*, **260**, 37–59.

SAADEH, S. 1982. *Ugharit, Mu'assaset Al-Fikr lil'abhath we Al-Nasher*, 1st edn. Beirut.

ŞAROĞLU, F., EMRE, Ö. & KUŞÇU, İ. 1992. *Active Fault Map of Turkey, 2 sheets*, Maden ve Tetkik Arama Enstitüsü, Ankara.

SBEINATI, M. R., DARAWCHEH, R. & MOUTY, M. 2005. The historical earthquakes of Syria: an analysis of large and moderate earthquakes from 1365 B.C. to 1900 A.D. *Annals of Geophysics*, **48**, 347–436.

SCHAEFFER, C. F. A. 1948. *Stratigraphie Comparée et Chronologie de l'Asie Occidentale (IIIe et IIe millenaires)*. Oxford University Press, Oxford.

SCHEFFERS, A. & KELLETAT, D. 2005. Tsunami relics on the coastal landscape west of Lisbon (Portugal). *Science of Tsunami Hazard*, **23**, 3.

SCHMIDT, J. 1879. *Studien über Erdbeben*. Carl Scholtze, Leipzig.

SHUTO, N., GOTO, C. & IMAMURA, F. 1990. Numerical simulation as a means of warning for near-field tsunami. *Coastal Engineering in Japan*, **33**, 773–793.

SIEBERG, A. 1932. Untersuchungen übar Erdbeben und Bruchscholenbau im Östlichen Mittelmeergebeit. *Denkschrifften der Medizinsch-Naturwissenschaft Gesellschaft zu Jena*, **18**, 161–273.

SMITH, W. H. F. & SANDWELL, D. T. 1997*a*. *Measured and estimated seafloor topography (version 4.2)*. World Data Centre-A for Marine Geology and Geophysics Research Publication **RP-1**.

SMITH, W. H. F. & SANDWELL, D. T. 1997*b*. Global seafloor topography from satellite altimetry and ship depth soundings. *Science*, **277**, 1957–1962.

SOLOVIEV, S. L., SOLOVIEVA, O. N., CHAN, N. G., KHEN, S. K. & SHCHETNIKOV, N. A. 2000. *Tsunamis in the Mediterranean Sea 2000 B.C.–2000 A.D.* Advances in Natural and Technological Hazard Research, **13**.

STIROS, S. C., MARANGOU, L. & ARNOLD, M. 1994. Quaternary uplift and tilting of Amorgos Island (southern Aegean) and the 1956 earthquake. *Earth and Planetary Science Letters*, **128**, 65–76.

TAHER, M. A. 1979. *Corpus des texts arabes relatifs aux tremblements de terre et autres catastrophes naturelles de la conquête arabe au XII H. /XVIII J.C.* Thèse de Doctorat d'Etat, Université Paris 1.

TAYMAZ, T., JACKSON, J. A. & WESTAWAY, R. 1990. Earthquake mechanisms in the Hellenic trench near Crete. *Geophysical Journal International*, **102**, 695–731.

TAYMAZ, T., JACKSON, J. A. & MCKENZIE, D. 1991. Active tectonics of the north and central Aegean Sea. *Geophysical Journal International*, **106**, 433–490.

TAYMAZ, T., WESTAWAY, R. & REILINGER, R. (eds) 2004. Active faulting and crustal deformation in the eastern Mediterranean region. *Tectonophysics*, (Special issue), **391**.

TAYMAZ, T., WRIGHT, T. J., YOLSAL, S., TAN, O., FIELDING, E. & SEYİTOĞLU, G. 2007. Source characteristics of the 6 June 2000 Orta–Çankırı (central Turkey) earthquake: a synthesis of seismological, geological and geodetic (InSAR) observations, and internal deformation of the Anatolian plate. *In*: TAYMAZ, T., YILMAZ, Y. & DILEK, Y. (eds) *The Geodynamics of the Aegean and Anatolia*. Geological Society, London, Special Publications, **291**, 259–290.

TEN VEEN, J. H., WOODSIDE, J. M., ZITTER, T. A. C., DUMONT, J. F., MASCLE, J. & VOLKONSKAIA, A. 2004. Neotectonic evolution of the Anaximander mountains at the junction of the Hellenic and Cyprus arcs. *Tectonophysics*, **391**, 35–65.

THEILEN-WILLIGE, B. 2006. Tsunami risk site detection in Greece based on remote sensing and GIS methods. *Science of Tsunami Hazard*, **24**, 35–48.

WESSEL, P. & SMITH, W. H. F. 1991. Free software helps map and display data. *EOS Transactions, American Geophysical Union*, **72**, 441, 445–446.

WESSEL, P. & SMITH, W. H. F. 1995. New version of the generic mapping tools released. *EOS Transactions, American Geophysical Union*, **76**, 329.

YALÇINER, A. C. & PELINOVSKY, E. 2007. A short cut numerical method for determination of periods of free oscillations for basins with irregular geometry and bathymetry. *Ocean Engineering*, doi:10.1016/j.oceaneng.2006.05.016, **34**, 747–757.

YALÇINER, A. C., ALPAR, B., ALTINOK, Y., ÖZBAY, I. & IMAMURA, F. 2002. Tsunamis in the Sea of Marmara: historical documents for the past, models for the future. *Marine Geology*, **190**, 445–463.

YALÇINER, A. C., PELINOVSKY, E., OKAL, E. & SYNOLAKIS, C. E. 2003. *Proceedings of the NATO Advanced Research Workshop on underwater ground failures on tsunami generation, modeling, risk and mitigation*, 23–26, May 2001. Intanbul. NATO Science Series.

YALÇINER, A. C., PELINOVSKY, E., TALIPOVA, T., KURKIN, A., KOZELKOV, A. & ZAITSEV, A. 2004. Tsunami in the Black Sea: comparison of the historical, instrumental and numerical data. *Journal of Geophysical Research*, **109**, C12023, doi:10.1029/2003JC002113.

YOLSAL, S. & TAYMAZ, T. 2004. Seismotectonics of the Cyprus Arc and Dead-Sea Fault Zone: Eastern Mediterranean. *EOS Transactions, American Geophysical Union*, **85**, Fall Meeting Supplements, Abstract T52B-06.

YOLSAL, S. & TAYMAZ, T. 2005. Potential source regions of earthquakes and tsunamis along the Hellenic and Cyprus arcs, eastern Mediterranean. *In*: TAYMAZ, T. (ed.) *International Symposium on the Geodynamics of Eastern Mediterranean: Active Tectonics of the Aegean Region*, 15–18, June 2005, Kadir Has University, İstanbul, Abstract Volume, Tübitak, İstanbul, Turkey, 240.

ZAHIBO, N., PELINOVSKY, E., YALÇINER, A. C., KURKIN, A., KOSELKOV, A. & ZAITSEV, A. 2003. The 1867 Virgin Island tsunami. *Natural Hazards and Earth System Sciences*, **3**, 367–376.